RADIOTECT

COOP-CT-2006-032744

RADIOTECT

Ultra Wideband Radio application for localisation of hidden people and detection of unauthorised objects

D25 Final Report

(Final Activity Report)

Start date of project: 01/01/2007 Duration: 30 months

Due date of deliverable: 14/08/2009 Actual submission date: 24/09/2009

Instrument: Cooperative research Thematic Priority: Horizontal research activities involving SMEs

Document Information	
Lead by:	TUI
Prepared by:	ALL
Reviewed by:	ALL
Security*:	PU
Protocol:	RA_FAR_D25
Rev.:	1.0
Date of issue	24/09/2009
Annex No.	

Project co-funded by the European Commission within the Sixth Framework Programme (2002-2006)

---

* **PU** = Public

PP = Restricted to other programme participants (including the Commission Services).

RE = Restricted to a group specified by the consortium (including the Commission Services).

CO = Confidential, only for members of the consortium (including the Commission Services).

SUMMARY: This is the publishable final report also representing the final activity report for the project.

It summarises the main project activities and results over the full duration of the project.

We describe the project objectives, participants, approach, work performed and results.

Document Evolution			
Revision	Date	File Reference	Reason of change
Rev. 0.1	17/03/2009	*RA_FAR_D25_0.1*	First structure and content
Rev. 0.2	16/06/2009	*RA_FAR_D25_0.2*	Update
Rev. 0.3	11/09/2009	*RA_FAR_D25_0.3*	Update
Rev. 0.4	20/09/2009	*RA_FAR_D25_0.4*	Update
Rev. 1.0	24/09/2009	*RA_FAR_D25_1.0*	First version

Contents

1 Project objectives, partners achievements

1.1 Objectives

The overall project objectives may be summarised as follows:

- To develop high and ultra high resolution radar hardware for the detection of hidden persons / objects for use in rescue and security applications
- To develop imaging techniques and algorithms for use with high and ultra high resolution radar for the detection and localisation of persons / objects for rescue and security applications
- To test the above technologies to help determine methodologies of use and room for further improvements.
- To improve the competitiveness of the SMEs in the project and the establishment of transnational cooperation
- To promote the technology to strengthen its commercial success. Products for rescue and security are foreseen.

1.2 Contractors

Type	***Name***	***Country***
Government Authority	Swedish Civil Contingencies Agency	Sweden
SME	MEODAT GmbH	Germany
SME	GEOZONDAS Ltd	Lithuania
SME	INGMETAL	Slovakia
SME	IRK-Dresden	Germany
SME	Crabbe Consulting Ltd	Germany
University	Vrije Universiteit Brussel	Belgium
University	Technická univerzita v Košiciach	Slovakia
University	Delft University of Technology	The Netherlands
University	Technische Universität Ilmenau	Germany

1.3 Summary of achievements

The overall achievements may be summarised as follows:

- A high resolution radar working with the M-Sequence technique has been developed to enable security forces to detect persons hidden behind walls. This was achieved through advances in the state of the art for radar electronics and algorithms for person detection and tracking.
- A high resolution radar also working with the M-Sequence technique has been developed to enable rescue forces to detect persons trapped under rubble. This was also achieved

through advances in the state of the art for radar electronics and algorithms for person detection and localisation.

- A further high resolution radar working with the sub-nano second impulse technique has been developed which demonstrates the ability to detect movement including heart beat and breathing also for security or rescue applications. This was also achieved through advances in the state of the art for radar electronics and algorithms for person detection and localisation.
- 3 systems working with the sub-nano second impulse radar technique up to 18 GHz were developed to investigate the challenge of imaging objects hidden behind clothes. This was also achieved through advances in the state of the art for radar electronics and algorithms for person detection and localisation.
- Components were developed utilising SiGe semiconductor chip and LTCC technology for a mm-wave radar to work in the frequency range 60-70 GHz. This was also achieved through advances in the state of the art for radar electronics.
- All systems have been tested in the laboratory and those closest to the market evaluated in tests with end users.
- The SMEs have results from the project which they assess as increasing their competitiveness. The SMEs estimate their economic benefit from the project will be as high if not higher than planned in preparing the project.
- Products for rescue and security application are foreseen and project results may be used in other application areas.
- The partners have developed strong and trusting working relationships with each other.
- There have been 41 scientific papers published (or will be published) at the time of writing on results from the project.

2 Detection of hidden people and objects by through wall imaging

2.1 The approach to detect moving people behind a wall

2.1.1 Target localisation based on tri-lateration

Classical radar devices use range measurements and rotating antennas with a pencil beam to locate the target. But, narrow beam antennas for low operational frequencies have huge geometrical dimensions, which cannot be handled by a single person under hazardous situations. Hence, we use a different conception. It applies small wide beam antennas and tri-lateration.

The tri-lateration principle is depicted in the Figure 2-1. The distances d_1 and d_2 are estimated by the radar sensors based on round trip time measurement. Since the coordinates of transmitting antenna ($Tx = [x_T, y_T]$) and receiving antennas ($Rx_k = [x_k, y_k], k = 1,2$) are known a-priory, the coordinates of the target ($T = [x, y]$) can be determined as an intersection of ellipses. It follows from the fact that each range d_k and the pairs Tx and Rx_k form two ellipses (E_1, E_2) with the foci $Tx = [x_T, y_T]$ and $Rx_k = [x_k, y_k]$ and with the length of the main half-axis $a_k = d_k / 2$. It can be found very easily, that the target lies just on the intersection of these ellipses (Figure 2-2). The target coordinates can be calculated as a solution of a nonlinear equation set by the direct calculation method. As the ellipses are expressed by the second order polynomials, there are two solutions for their intersections. However, there is only one solution corresponding to the true coordinates of the target. Therefore, one of the obtained solutions has to be excluded for the scenario with one target. Usually, one solution is eliminated based on the fact that the half-plane where the target is located is known in advance.

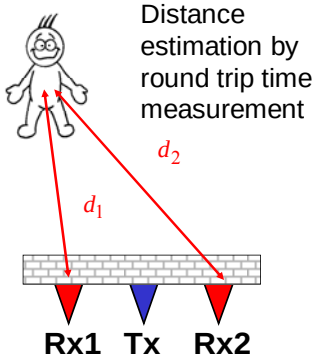

Figure 2-1: The principle of person localisation by tri-lateration.

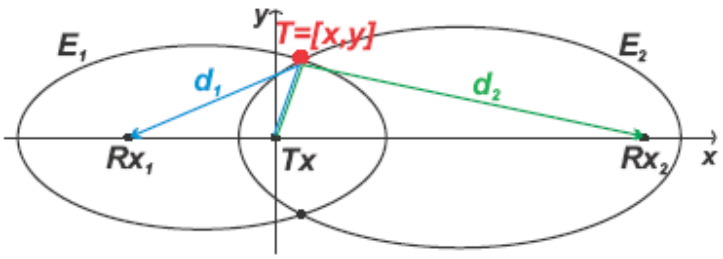

Figure 2-2: Target localisation based on tri-lateration.

2.1.2 Scanning for SAR-processing

SAR is a back-projection (or stack migration) imaging method that was first developed for airborne radar applications. UWB radar transmits (after despreading) a short impulse which is reflected by an object and received back by the radar. Such a received reflection in a discrete time *n* is called an A-scan and the position of the impulse in the discrete time domain corresponds to the position of the object in space. In order to obtain more information about the investigated objects and to narrow antenna flaring angle beam, the SAR scanning is applied.

The basic 2D SAR spatial model is shown in Figure 2-3 a). A transmitted wave is reflected from the target to all directions uniformly. As the antenna beam is wide, the signal reflected from the target is received not only when the antenna system is exactly over the target, but in many positions that allow ”seeing” the target. This will cause that one point in S(X;Y) space will be represented in an acquired B-scan (set of A- scans assembled

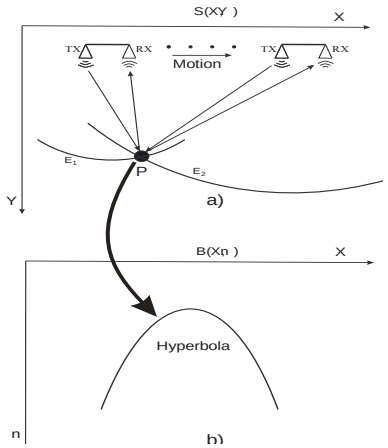

Figure 2-3: Fig.1 SAR scanning principle

together in a 2D structure) as a hyperbola, as it is show in Figure 2.3 b). The X is scanning direction and Y is the looking direction.

Processing of SAR scanned signals was used mainly for visualization (imaging) of large object behind walls.

2.2 The radar electronics

The radar electronics consists of two main parts:

- the Radar Head RF electronics
- the Radar processing unit

2.2.1 Radar head RF electronics

The RF electronics is implemented with the improved UWB chipset designed and developed by MEODAT and TUI. The main parts are

- one transmitting channel
- two receiving channels
- one clock unit
- RF amplifiers with base band low pass filters
- power supply circuits for the chip electronics

The complete RF electronics is implemented in a new type of RF housing developed and manufactured by MEODAT, TUI and INGMETAL.

2.2.2 Radar processing unit

The radar processing unit consists of a high integrated PCB:

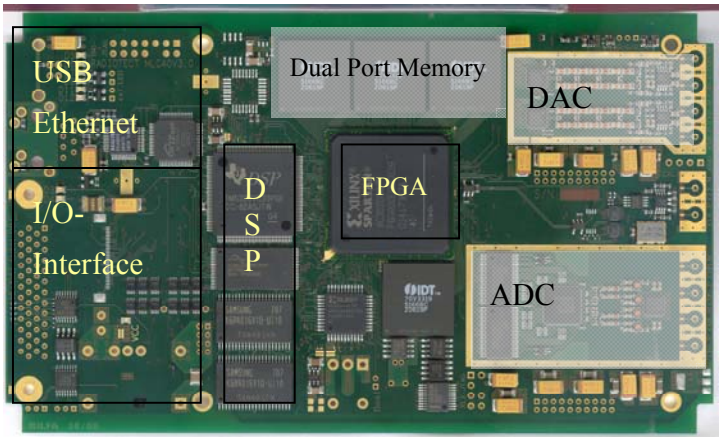

Figure 2-4 Radar processing unit

The functional blocks of the radar processing unit are:

- Dual channel fast ADC (14 Bit, up to 48 MHz sampling rate)
- Dual channel fast DAC (14 bit, up to 48 MHz sampling rate)
- Clock interface
- Dual channel slow DAC (16 bit, for feedback sampling application)
- Real time dual port memory for ADC and DAC
- FPGA for fast data acquisition and processing
- DSP system for fast data processing
- Ethernet- and USB interface
- IO-Interface for RF control, positioning system

2.2.3 Antenna

2.2.3.1 Antenna design and simulations

Spiral Antenna

- size: Ø 165mm, deep 30mm
- mass ca. 300g
- material: brass, TMM6
- matching 500 MHz – 4 GHz
- coupling level between neighboring elements : 32 dB

Figure 2-5: Spiral antenna

2.2.4 Casing

2.2.4.1 Construction of the Casing

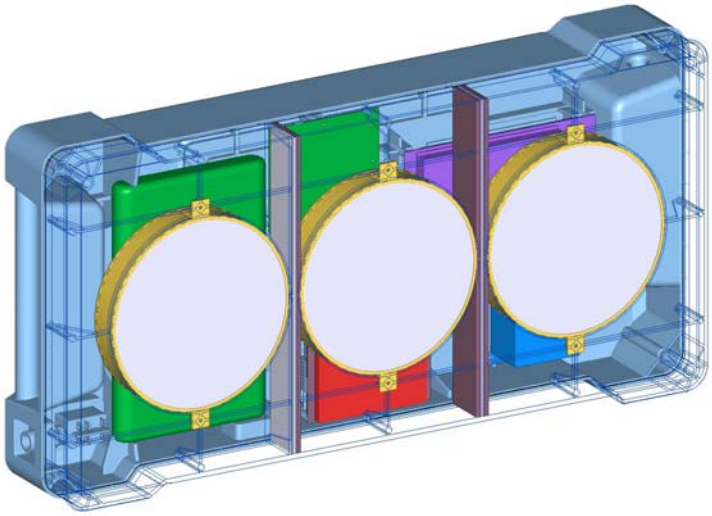

Figure 2-6 Casing 3a front view

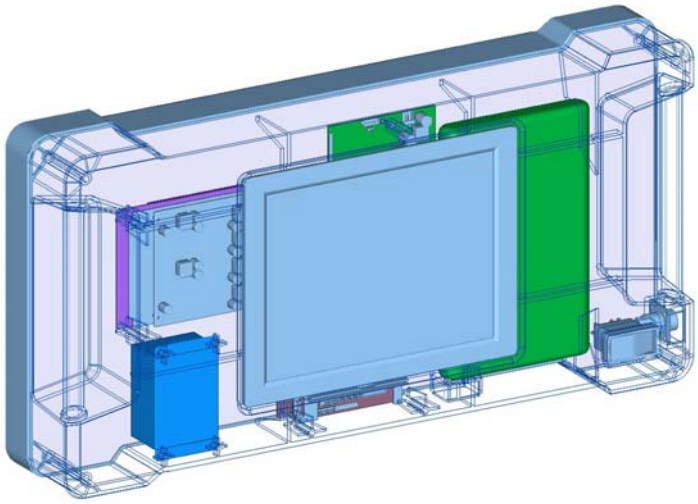

Figure 2-7: Casing 3b back view

2.2.5 Prototypes

The following figures show some photographs of the two prototypes:

Figure 2-8: Prototype 1, back view

Figure 2-9: Prototype 1, front view

Figure 2-10: Prototype 2, back view

Figure 2-11: Prototype 2, front view

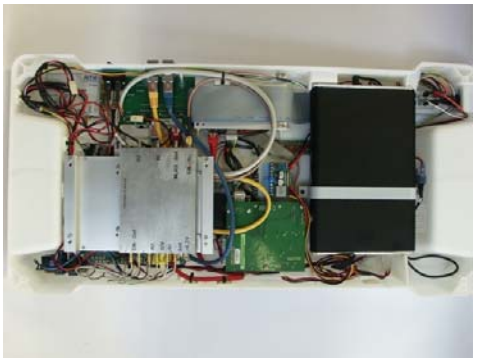

Figure 2-12: Internal view (electronics, internal accumulator)

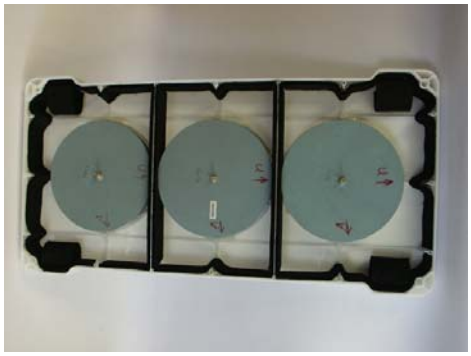

Figure 2-13: Internal view (antenna without backside shielding)

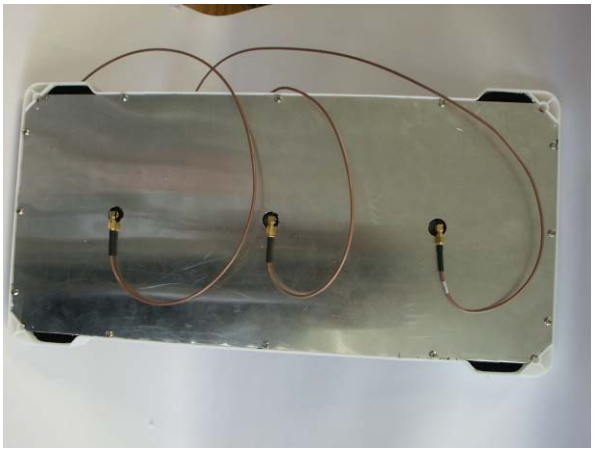

Figure 2-14: Internal antenna backside shielding

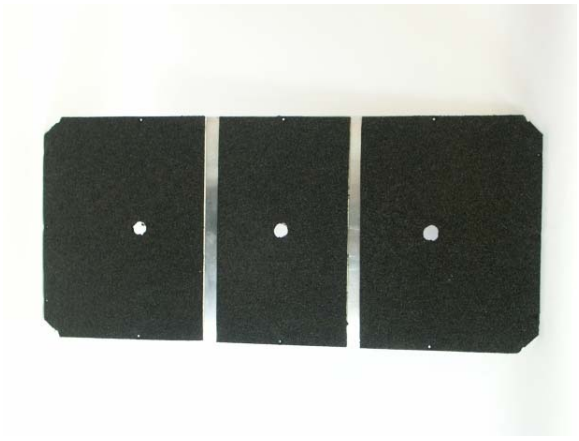

Figure 2-15: Internal antenna backside absorber

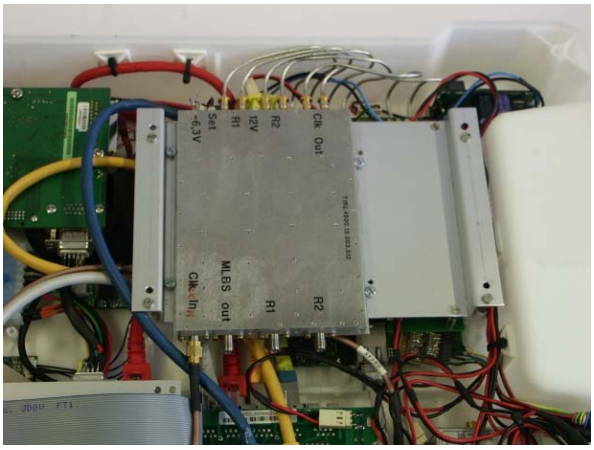

Figure 2-16: RF radar electronics

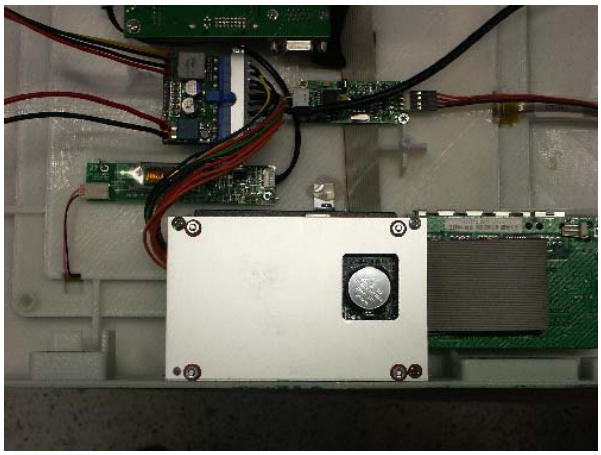

Figure 2-17: Internal PC system (Micro-PC)

Figure 2-18: Internal Flash Disk (4 GB)

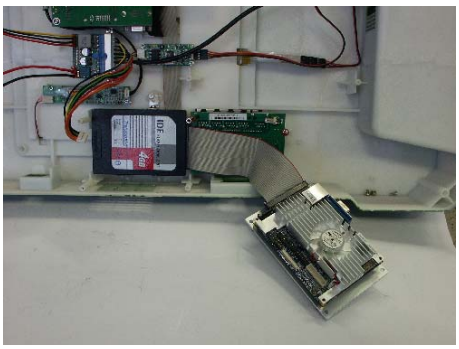

Figure 2-19: PC system (top)

2.3 Radar processing

2.3.1 Through wall tracking of moving target

There are two basic approaches for through wall tracking of moving targets. The former approach is based on radar imaging techniques, when the target locations are not calculated analytically but targets are seen as "hot spots" in gradually generated radar images. For the radar image generation, the different modifications of back projection algorithms can be used. With regards to the fundamental idea of the method - the radar image generation based on raw radar data, the method is usually referred to as *the imaging method*. In the case of the imaging method, moving target tracking (i.e. determining of target coordinates as the continuous function of time) is the complex process that includes the following tasks of radar signal processing: raw radar data pre-processing, background subtraction, fusion of data obtained from the radar receiving antennas, detection, localization and tracking itself.

In the case of the later approach, the target coordinates are evaluated by using time of arrival (TOA) corresponding to targets to be tracked and electromagnetic wave propagation velocity along the line transmitting antenna-target-receiving antenna. Moving target tracking based on TOA

estimation is the signal processing procedure that consists of the following phases of radar signal processing: raw radar data pre-processing, background subtraction, detection, TOA and target trace estimation, wall effect compensation, localization and tracking itself. Because TOA values taken on the corresponding observation time instances form so-called target trace, this method is referred to as *the trace estimation method*.

In the first phase of the RADIOTECT project which focused on through wall tracking of single moving targets, we tested and compared the performance of both above outlined methods. We found that both methods can provide very similar ability to estimate the moving target trajectory, including the accuracy of the target trajectory estimation. With regard to that fact, in the next step, we compared also the computational complexity and robustness of these methods. As the imaging method is based on image processing (2D signals) and the trace estimation method uses almost only 1D signal processing methods, we found that the computational complexity of the imaging methods is much higher than that of the trace estimation method. Besides, the results of radar signal processing for a number of scenarios for through wall tracking of a single target have confirmed that the trace estimation method is very robust, i.e. it can provide very stable and good results for different scenarios at the same setting of the parameters controlling the method performance. With regard to the comparison of the quality of performance, computational complexity and robustness of the imaging and trace estimation methods, we decided that the trace estimation method would be implemented in the radar prototype representing one of the RADIOTECT project outputs. Therefore, we will deal with the trace estimation methods only in the next part of this report.

Based on a number of measurements with the UWB radar, we have found that for some very complex scenarios, the application of a single UWB radar system equipped with one transmitting and two receiving antennas does not provide very good results for through wall tracking of moving targets. Under these circumstances, the target trajectory estimation can be improved by the application of cooperative positioning by using two independent UWB radar systems. Here, the signal processing phases of the conventional trace estimation method from the signal preprocessing phase up to the TOA estimation phase and the same tracking algorithms can be used. Due to the different number of antennas and their different layout, the target localization problem statement for cooperative positioning is different than that for localization based on a single UWB radar system equipped with one transmitting and two receiving antennas. It means, that if the target localization phase by the direct calculation method applied for the scenario with a single UWB radar system is replaced by the method of joining intersections of the ellipses with a decision algorithm (SPE), the trace estimation method modified in such a way can also be applied with success for two independent UWB radar systems used for target tracking.

2.3.2 Large Objects: wall parameter estimation, chain of data processing

Large static objects imaging is based on SAR migration. Before SAR migration can be applied, several preprocessing and calibration steps must be undertaken, such as: oversampling, time zero estimation, crosstalk removing and deconvolution. This preprocessing is necessary for imaging of objects behind the wall and it greatly improves the resultant image. For the case of through-wall imaging, the focused image of the object distribution is given in the same form as in standard SAR airborne application methods. However, due to the presence of the wall, with different dielectric constants, the travel paths of the signal from the emitting antenna (TX) to the point P and from the point to the receiving antenna (RX) are not straight lines as in free space as shown in Figure 2-20. Therefore the Time of Arrival (TOA) must be calculated based on Snell's law.

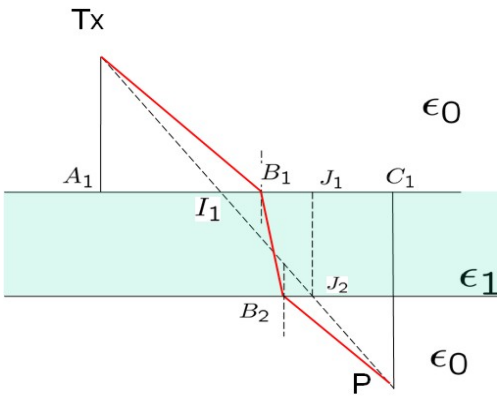

Figure 2-20: Travel path of the signal in a three-layered medium

The TOA between the antennas and the points in multilayered media are not easily calculated. It must be determined using some optimization procedures which are based on the principle of minimal travel time. Since the minimization must be applied to all points, the computation becomes very time-consuming. Moreover wall parameters (mainly dielectric permittivity and wall thickness) are usually not known in advance and must be estimated in order to use this approach.

A special calibration procedure for estimation of these parameters by hand-held UWB radar was proposed and optimized for the through wall measurement scenario.

An efficient TOA estimation algorithm for air-wall-air was developed and used for through wall imaging.

2.4 Examples

2.4.1 Through wall tracking of moving people

The performance of the trace estimation method outlined in the Section 2.3 for through wall tracking of moving targets will be illustrated by using three fundamental scenarios. It is *the scenario Tile-2d* which focused on the tracking of two moving targets, *the scenario Concrete-1d* illustrating wall effect compensation significance as well as *the scenario Cooperative positioning* indicating the potential of cooperative position of a target by using two independent UWB radar systems.

The scenario Tile-2d is outlined in the Figure 2-21- Figure 2-23. In this scenario, two persons were walking in the gymnasium - the first person from the position P1.1 to the position P1.2 and the second person from the position P2.1 to the position P2.2 (Figure 2-21). The wooden wall was covered by tile and it had a thickness of 24 cm (Figure 2-22). The raw radar data were acquired by means of the M-sequence UWB radar with one transmitting and two receiving channels. The transmitting antenna (Tx) was located in the middle between two receiving antennas (Rx1, Rx2).

The distance between adjacent antennas was set to 1.3 m. During measurement, all antennas were placed on the bench (Figure 2-22). For the radar signal processing, the trace estimation method outlined in the Section 2.3 has been used. Here, zero-time setting using signal cross-talk, exponential averaging, CFAR detector, the trace connection method, the direct calculation method and multiple target tracking system based on linear Kalman filtering were used for signal preprocessing, background subtraction, target detection, TOA and trace estimation, localization and tracking, respectively. The trajectory estimations of the targets for the scenario Tile-2d are given in the Figure 2-24. Here, the trajectory estimation of the first and the second target are drawn by the read and black thick curve, respectively. It can be seen from this figure that the shapes of both estimated trajectories are very close to the true trajectories. This final result of the signal processing for the scenario Tile-2d confirms and illustrates the ability and the potential of the proposed trace estimation method for through wall tracking of multiple targets by using the M-Sequence UWB radar.

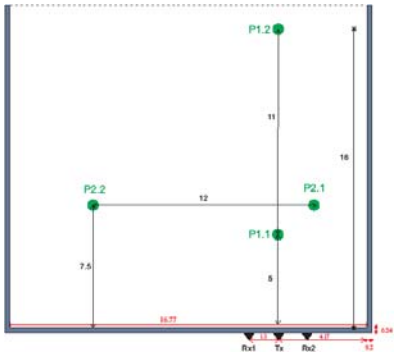

Figure 2-21: Scheme of scenario Tile-2d.

Figure 2-22: Scenario Tile-2d: exterior the building exterior.

Figure 2-23: Scenario Tile-2d: interior the building.

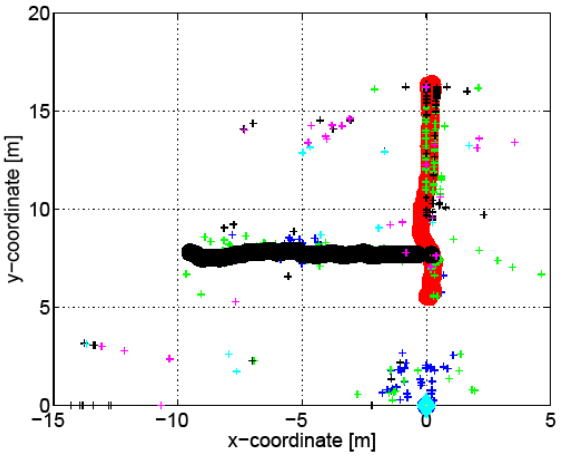

Figure 2-24: Scenario Tile-2d: The target trajectory estimations.

In order to illustrate the wall effect compensation significance, let us assume the scenario Concrete-1d outlined in the Figure 2-25. In this scenario, the target has been represented by a person walking along the perimeter of a rectangular room with size 3.9 m x 2.6 m, from Pos.1 through Pos. 2, Pos. 3 and Pos. 4 to Pos. 1. The walls of the room were made from concrete with thickness of 0.5 m and 0.27 m, relative permittivity $\varepsilon_r = 5$ and relative permeability $\mu_r = 1$. The raw radar data were acquired by means of the M-sequence UWB radar. The true target trajectory and the target trajectory estimated by the signal processing procedure described for the scenario Tile-2d including wall effect compensation by using the second order correction method are given in the Figure 2-26. In this figure, the true target trajectory is drawn by the red dash-dot curve, the target trajectory estimated by the localization phase is given by the blue thin dotted curve, the target trajectory estimated by Kalman filtering without wall effect compensation is represented by the blue thick dotted curve and finally, the target trajectory estimated by Kalman filtering with wall effect compensation is drawn by the black solid curve. It can be seen from these figures that the application of the wall compensation effect method for the scenario Concrete-1d leads to an expressive improvement of the target trajectory estimation in comparison with that obtained without the application of the wall compensation approach.

In the case of the wall effect compensation it is assumed that the wall parameters (permittivity and permeability of wall material, wall thickness) have to be known a priori, which is the most important limitation of the methods application. However, this restriction can be overcome by applying a new approach of wall parameter estimation based on measurements with the same UWB radar, which is applied for target tracking. This method has been developed within RADIOTECT project as well.

It follows from the physics of the wall effect, that the influence of the wall decreases if the transit time of the wave through the wall is small compared to the overall round trip time. For example, in the case of the scenario Tile-2d, the ratio between round trip time and wall transit time is relatively high, and therefore the wall effect was negligibly small. Hence, we were not forced to apply the wall effect compensation method in the scenario Tile-2d.

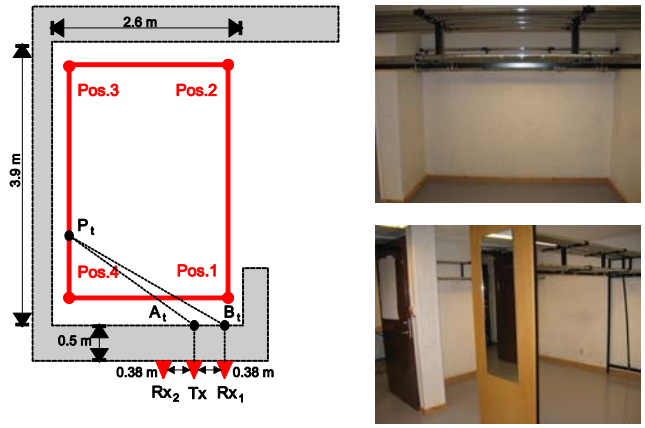

Figure 2-25: Scenario Concrete-1d. The scheme of the scenario and the pictures of scanned area.

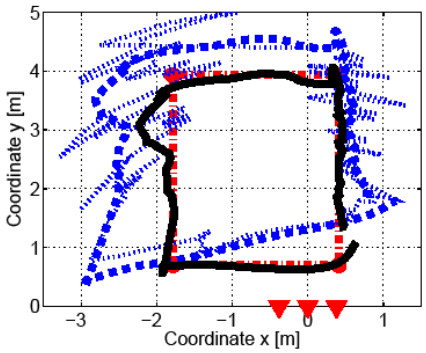

Figure 2-26: Scenario Concrete-1d: target trajectory estimations.

The scenario Cooperative positioning illustrates the performance of the modified version of the trace estimation method applied for through wall tracking of a moving target by using two independent radar systems. This scenario is outlined in the Figure 2-27. The target has been represented by a person walking from Pos.1 through Pos. 2 and Pos. 3 to Pos. 4. The walls of the room were made from bricks with thickness of 0.43 m and 0.3 m. The raw radar data analyzed in this example were acquired by means of two M-sequence UWB radars (radar system A - RSA and radar system B - RSB). The antenna lay-out of the radars is outlined in the Figure 2-27. The target trajectories estimated by RSA (green curve - LKF MPE RSA), by RSB (blue curve - LKF MPE RSB) and by using cooperative positioning (red curve - LKF MPE SPE) are given in the Figure 2-28. For the trajectory estimation by RSA and RSB, the signal processing procedure described for the scenario Tile-2D has been used. In the case of the trajectory estimation obtained from the fusion of data measured by RSA and RSB, the same procedure has been used. However, instead of the direct method of localization, the SPE has been applied for the target positioning. In the case of all trajectories, the linear Kalman filter (LKF) has been used for target tracking. The comparison of the true and estimated trajectories has shown very clearly, that cooperative positioning (the fusion of data measured by RSA and RSB using SPE method) can provide better target localization and tracking than that provided by RSA or RSB separately. The results obtained for the scenario Cooperative positioning should be considered to be only an introductory study demonstrating the performance of the basic method of the fusion of data obtained from two independent radar systems. We believe that the outlined approach of cooperative positioning has really the great potential, which can be exploited with advantage also in the field of multiple target tracking.

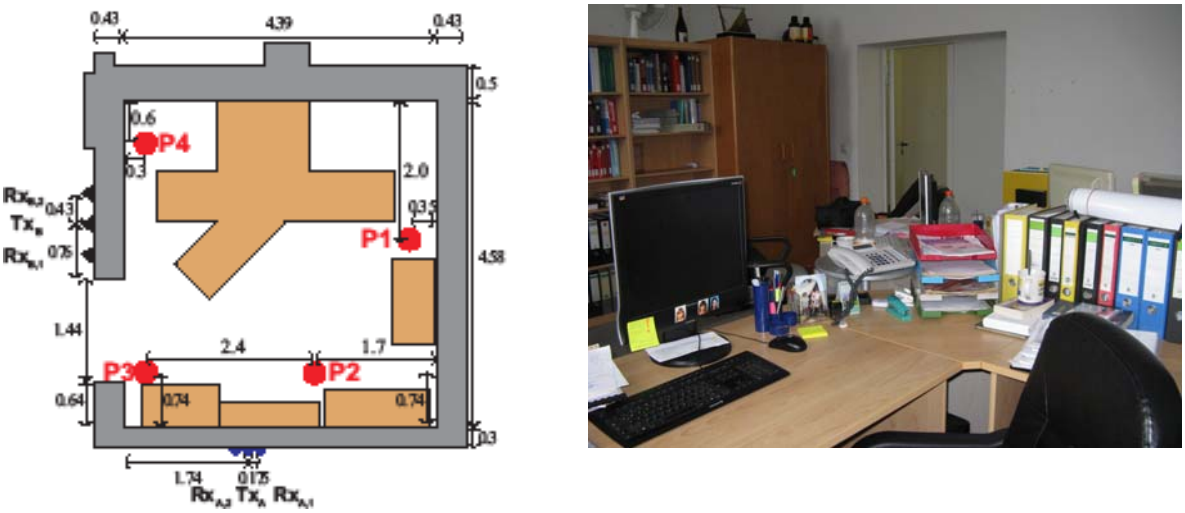

Figure 2-27: Scenario Cooperative positioning. The scheme of the scenario and the pictures of the scanned area.

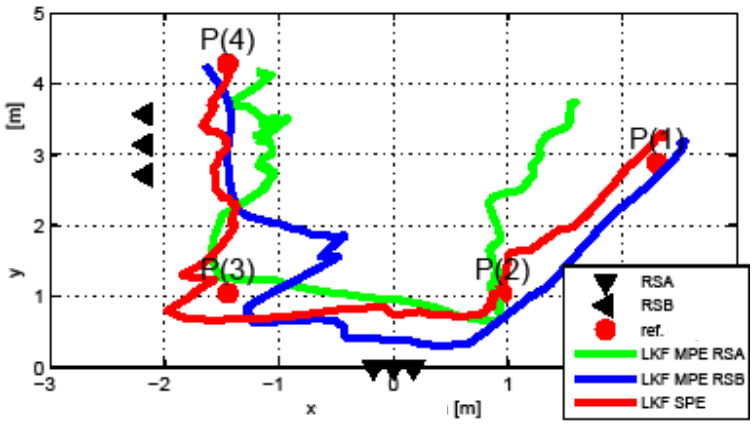

Figure 2-28: Scenario Cooperative positioning: target trajectories estimated by RSA, RSB and SPE

In the Section 2.3 of the Report, we have presented the novel procedure of radar signal processing for through wall tracking of moving targets by the M-Sequence UWB radars. This procedure can be applied for single as well as for multiple target tracking. We have shown that if the direct method of target positioning applied within the localization phase of the procedure is replaced by the method of joining intersections of the ellipses with a decision algorithm (SPE), the same procedure can be applied for target tracking by two independent radar systems as well. The procedure's performance has been demonstrated by the UWB radar signal processing for the three fundamental scenarios corresponding to single and two target tracking, as well as to target tracking by two independent radar systems (cooperative positioning). The obtained results have shown that

the proposed radar signal processing procedure can provide a good estimation of the target trajectories for all analyzed scenarios.

2.4.2 Through wall imaging of large objects

Large static objects and room (or building) contours are important and practical information that can be acquired from UWB scanning of static objects. The next figures summarize some practical results of UWB SAR based processing.

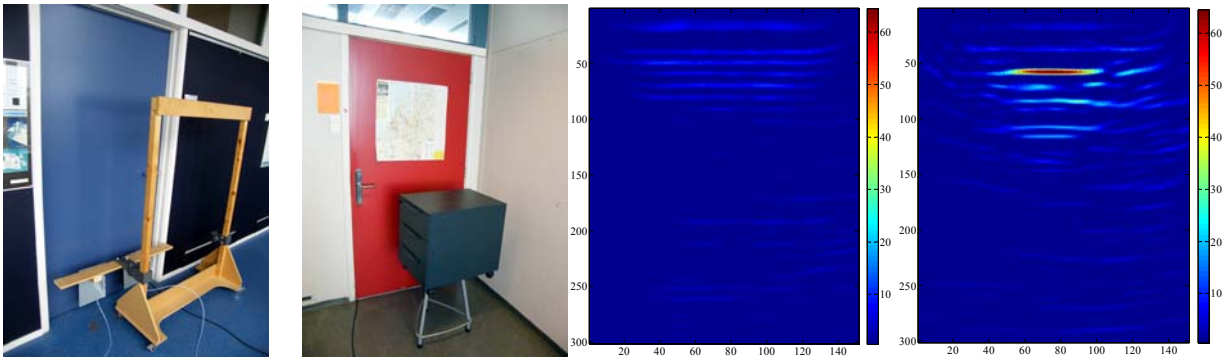

a) **b)** **c)** **d)**

Figure 2-29: Through door SAR scanning: a) Scanning system, b) Metal cabinet behind the door c) Imaging of empty room, d) Imaging of metal cabined behind the door

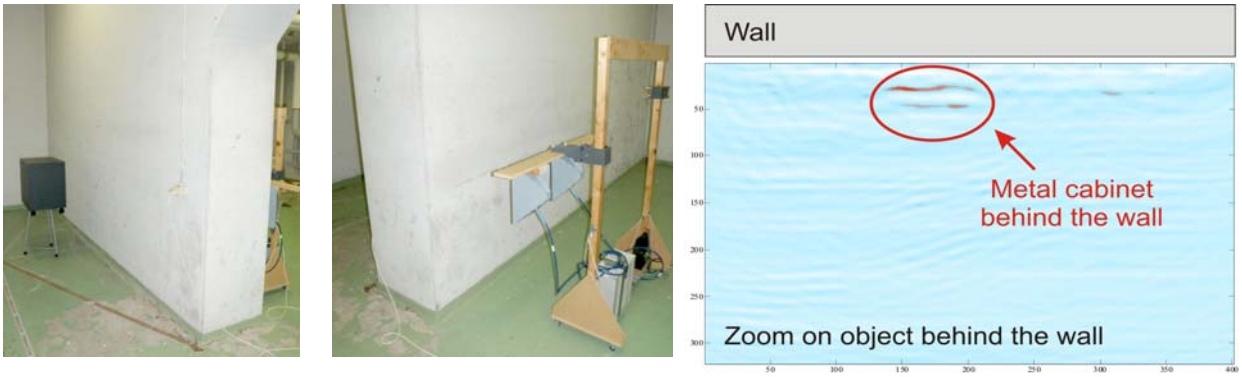

a) b) c)

Figure 2-30: Through 60 cm concrete wall SAR scanning: a) Metal cabinet behind the wall, b) Scanning system, c) Imaging and detection of metal cabined behind 60 cm concrete wall

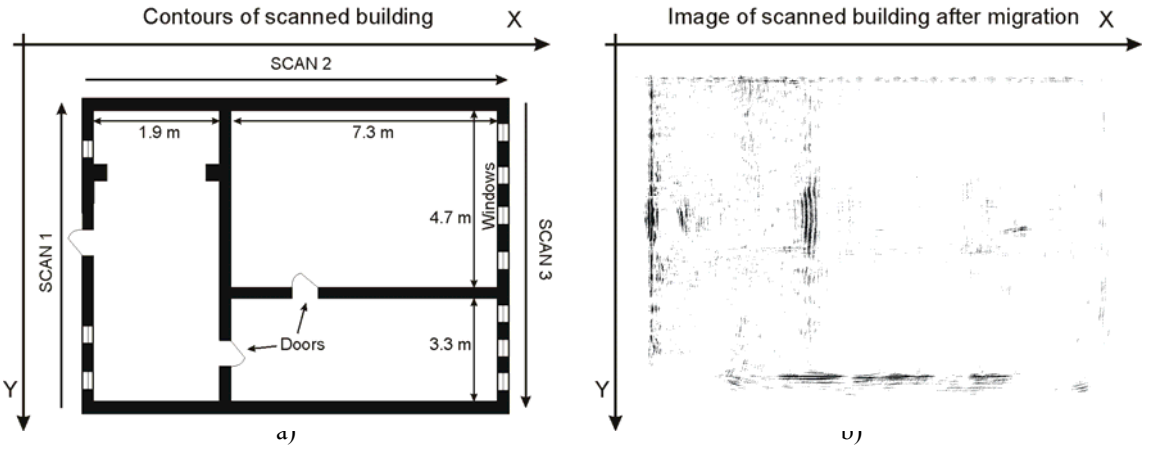

Figure 2-31: Building contours imaging a) SAR scanning of a building from 3 sides, b) migrated image of building contours from 3 SAR scans

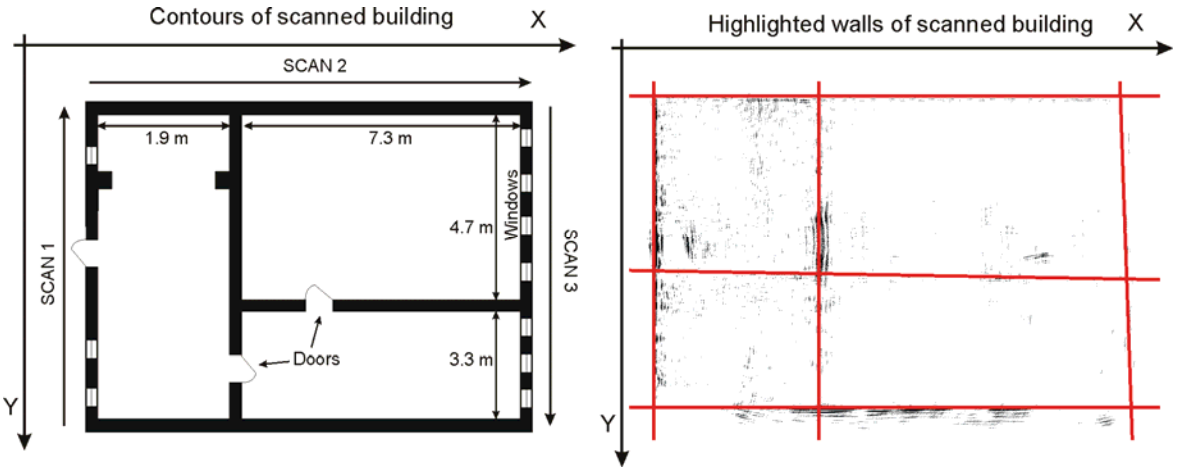

a) b)

Figure 2-32: Enhancing of building contours a) SAR scanning of a building from 3 sides, b) enhancing of building contours by filtration of migrated image in Hough space

3 Detection of unauthorised objects beneath clothes

3.1 The basic approach

The partners in the project have the vision to build a body scanner for the detection of unauthorised objects beneath clothes in the operational frequency ranged to about 60 … 70 GHz. Ultra-high resolution radar systems (bandwidth 8 GHz or more) at that frequency are not available at the moment and it is was out of the scope of this project to build and test such a radar within the given timeframe. We investigated the challenges of body scanning at a lower frequency i.e. 10-18 GHz in order to reduce the risk of the development of a 70 GHz system. During the project 3 through dress imaging (TDI) in the lower frequency range were developed and tested. In parallel we also developed mm-wave components based on SiGe-semiconductor technology which could lead to an integrated 60…70 GHz system.

The TDI synthetic aperture radar (SAR) system with mechanical scanner allows the imaging of objects. The quality of images is approximately the same in the frequency bands 3.1 – 10.6 GHz and 10 – 18 GHz. The scanning procedure requires however a great deal of time (1.5 – 3 hours) which is too long to scan a man. The present prototype can be applied for data collection to examine measurement procedures and algorithms for imaging using dolls, pigs and etc.
A second TDI system using a fixed antenna array (MIMO-System) allows the imaging of objects in free space, but not close to the bodies of dummies with strongly reflecting metal surfaces. The task can be solved by the use of a TDI SAR-MIMO system including an antenna array and a scanner. However at the present time, the scanning procedure takes also too long. It requires 12 s to scan a portion with a height of 40 cm. For practical application of this prototype it will be necessary to extend the pulse repetition frequency of the sampling converter and pulse generator up to 10 MHz. That would allow for the reduction of the scanning time to 5 s for a body of 2 m height. Geozondas Ltd. intends to include such a development project in its plans.

Imaging has been fulfilled in the frequency bands 3.1 – 10.6 and 10 – 18 GHz. The quality of images in both bands is almost similar. The frequency band 3.1 – 10.6 GHz is assigned in the standards of Europe (not totally) and of the USA for radar imaging, however for security and rescue application exceptions are acceptable.

In the images made in the frequency band 10 – 18 GHz, the hidden objects are clear visible. The image of the person's body has no optical quality so there are no ethical problems which arise when scanning with mm-wave radars is performed ("naked man" imaging). An axe, a gun, and a knife have been imaged with reasonable quality as have large and smaller metal weapons on the human body. A medium-sized plastic anti-personnel landmine has also been imaged successfully as a dielectric weapon on the human body.

3.2 The radar electronics

3.2.1 Evaluation system up to 18 GHz

3.2.1.1 Introduction

Three different TDI radar systems were designed, built and tested.

One of TDI systems is a 2-D SAR, the other is based on a MIMO 2D array radar and the third system represents a combination of the linear MIMO array and 1-D SAR (MIMO-SAR). The 2-D SAR includes a pair of transmit (Tx) and receive (Rx) antennas mounted on a 2-D mechanical scanner that moves the antennas in small steps within a given aperture. A small step size provides a low level of artefacts in the focused image but on the other hand it makes scanning too slow.

The MIMO array acquires the data much faster and as such it is intended for practical use but the focused image can have significant artefacts due to the relatively large separation between the array antennas. The MIMO-SAR makes use of a linear MIMO moved by the scanner in the vertical direction with a small step size, which results in much lower artefacts and a reduced scanning time.

3.2.1.2 High precision mechanical scanner

A high precision mechanical scanner is an essential part of a TDI SAR system. The scanner moves antennas as well as the remote electronics modules: sampling unit and pulse generator head. The scanner has been assembled from modules and components purchased from Isel Automation GmbH, Germany. The computer control has been realized by means of the Scanner Controller from Isel Automation. Placing the sampling unit and the pulse generator head near the antennas, we avoid losses in the RF cables. For linear motion in X-Y of the mechanical scanner we use ball screw spindle units. The scanner is placed on a special metallic table (Figure 3-1).

Figure 3-1: Mechanical scanner with three movable antennas

The scanner is controlled by dedicated software which can move the radar over an arbitrary trajectory.

3.2.1.3 UWB electronics

The electronics has been built on a video impulse technology with sequential (stroboscopic) sampling. A detailed description can be found in deliverables D3 and D11. Shortly, the electronics consist of a transmitter, receiver and computer with dedicated signal processing and visualization software.

The transmitter represents a pulse generator head and a control/triggering device or mainframe (Figure 3-2). The pulse generator head fires a mono-pulse with 30 ps duration while TTL triggering, power and signal time delay are provided by the mainframe. The pulse generator is used in all described systems.

Figure 3-2: Pulse generator mainframe and head

Two kinds of receiver providing a bandwidth from DC to more than 30 GHz were used in TDI measurements. One is a two-channel sampling converter that works with two Rx antennas simultaneously (Figure 3-3) in SAR and systems for vital data capturing.

Figure 3-3: Two-channel sampling converter with sampling unit

The second receiver device covers eight channels (Figure 3-4) and it was used in SAR and MIMO array systems.

Figure 3-4: Eight-channel sampling converterr

The UWB multiplexer (Figure 3-5) includes one switch 1→4 to connect the generator head and transmitting antennas and eight switches 1→2 to connect the receiving antennas and 8-channel sampling converter inputs in the MIMO and MIMO-SAR radar systems.

Figure 3-5: UWB multiplexer

3.2.1.4 1-30 GHz pulse radiated antenna

A double-ridged TEM horn antenna with lens GZ0126DRH-2 has been designed by Geozondas for imaging, breathing and heart beat detection in a frequency band from 1 to 30 GHz. The antenna is shown in Figure 3-6.

Figure 3-6: TEM horn antenna

The antenna dimensions are 90 x 120 mm for the aperture and 310 mm in length, while the weight is 650 g.

3.2.1.5 10-18 GHz antenna

TUD developed an UWB antenna 10 -18 GHz for the TDI radar that represents a stacked patch antenna (Figure 3-7). Such an antenna is reasonably simple manufactured and has planar geometry, it radiates only in one hemisphere with a sufficiently large beam width, and the pulse distortion is acceptable.

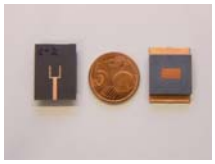

Figure 3-7: Stacked patch antenna (back side, coin for comparison, front side)

3.2.1.6 SAR with mechanical scanner

A SAR imaging system (Figure 3-8) was designed and assembled at Geozondas.

(a)  (b)  (c) 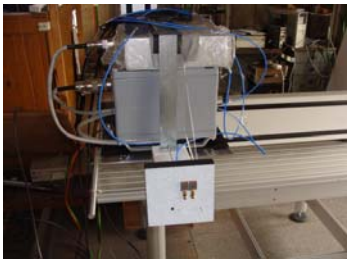

Figure 3-8: SAR imaging System with mechanical scanner

(a) with antennas 1 -30 GHz; (b) with antennas 3.1 – 10.6 GHz; (c) with antennas 10 – 18 GHz

The system includes:

- 2-channel Sampling converter
- Pulse Generator mainframe and head
- 1 transmitted and 2 or 3 pulse radiated antennas
- Mechanical scanner

3.2.1.7 3.1 – 10.6 GHz and 10-18 GHz MIMO array

The MIMO 2D array (Figure 3-9) was designed at TUD and assembled at Geozondas. It consists of four Tx- and sixteen Rx-antennas. The Tx-antennas work sequentially while all sixteen receiver antennas capture the waves simultaneously.

(a) 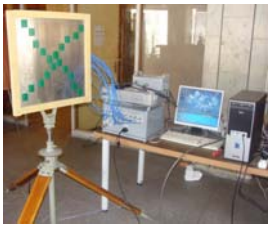 (b) 

Figure 3-9: MIMO array system in Geozondas

(a) With 2D array 3.1 – 10.6 GHz; (b) With 2D array 10 – 18 GHz

The system includes:

- 8-channel sampling converter;
- pulse generator (generator head and mainframe connected with cable);
- MIMO array (antennas are fixed on a common plate);
- UWB multiplexer (switch 4:1 for Tx-antennas and 8 switches 2:1 for Rx-antennas, placed in one case).

3.2.1.8 10-18 GHz MIMO-SAR

A MIMO linear array (Figure 3-10) was designed at TUD and assembled at Geozondas. It consists of four Tx- and sixteen Rx-antennas. Also here, the Tx-antennas work sequentially while all sixteen receiver antennas capture the waves simultaneously. The linear MIMO array moved by the scanner in the vertical plane represents a combined MIMO-SAR system.

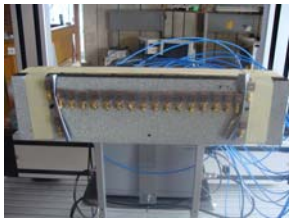

Figure 3-10: MIMO-SAR system: array installed on scanner

3.2.2 mm-wave components

The intention of the work was to develop basic principles and technologies for a low cost mm-wave radar front end for near field imaging purposes. Such a system is built from a large number of radar channels, i.e. a sensor array, which are distributed over a certain area. Depending on the intended use the array operates in a stationary way or it is hand held. Hence, production cost of the electronics, their weight, size and power consumptions are important issues of the overall conceptions.

We proposed and investigated the system as depicted in Figure 3-11 (see also [1]). It is based on an M-sequence base band system, which operates at a clock rate of about 9.4 GHz. This provides a usable bandwidth of 4.7 GHz. In a first intermediate stage this signal is mixed up to a frequency band 9.4±4.7 GHz and finally in a second step to the wanted mm-wave band 65.4±4.7 GHz. On the receiver side, the signal is down converted by the same schematics using a sequential IQ-demodulator in the IF stage.

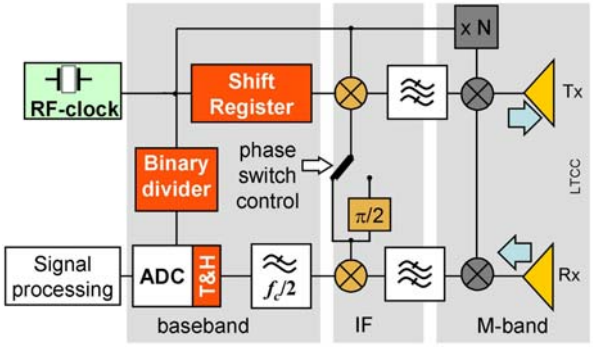

Figure 3-11: Ultra-wideband mm-wave radar front end

The final goal is a full monolithic integration of the whole radar front end. This project dealt with the integrations of the mm-wave front end. For experimental and development purposes, the active

components, i.e. up-converter and power amplifier, the down-converter plus low noise amplifier and the beat signal generator (see Figure 3-12), were manufactured on individual chips and mounted on a LTCC-carrier.

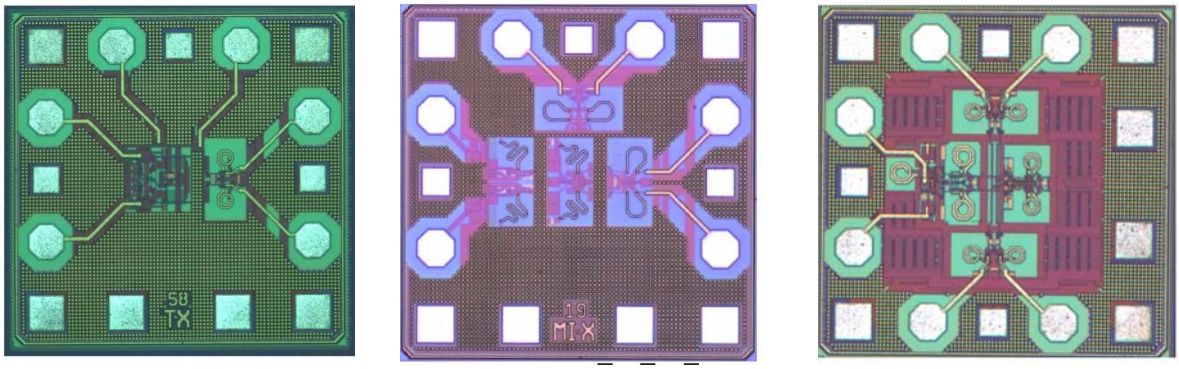

mm-wave up-converter die | mm-wave down-converter | beat signal generation die

Figure 3-12: Micrographs of the active key components of the mm-wave up-down converter.

In order to avoid long feeding cables for mm-wave signals, the antennas were integrated onto LTCC-substrates. The LTCC-technique permits the building of three dimensional electrode structures so that complicated antenna geometries can be implemented which are directly fed by the integrated circuits. Figure 3-13 depicts the structure of the developed antennas. The complete implementation of a test sample of the up-down converter is shown in Figure 3-14.

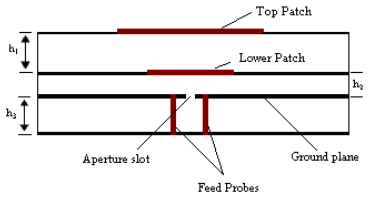

Side view

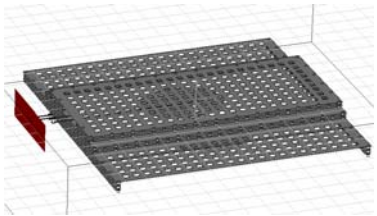

Perspective view of the antenna shield. The radiators are placed at the bottom.

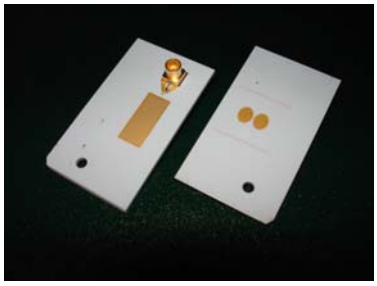

Photo of a test sample:

left upper side with shielding and RF-connector, right: lower side with the symmetric radiators

Figure 3-13: Example of integrated antennas [2], [3]

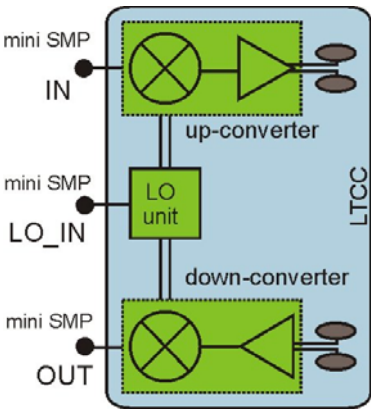

Block schematic

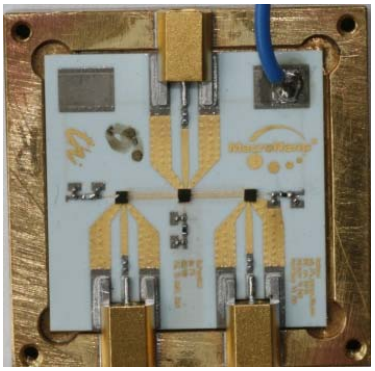

The side with the active components

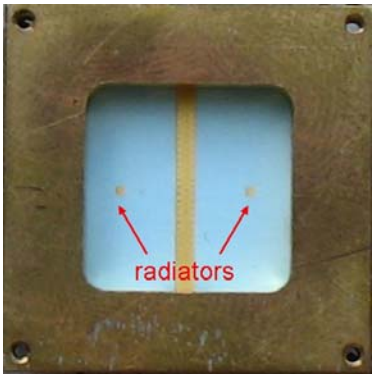

The radiator side

Figure 3-14: Schematic and photo of an assembled mm-wave up-down-converter manufactured at LTCC-substrate.

Reference
[1] M. Kmec, J. Müller, P. Rauschenbach, S. Rentsch, J. Sachs, B. Yang: Integrated cm - and mm-Wave UWB Transceiver for M-Sequence Based Sensors. EUROEM 2008, 21-25 July, Lausanne, Switzerland. Will be published in Ultra-Wideband, Short-Pulse Electromagnetics 9
[2] Y. A. Kirana, A. G. Yarovoy, L. P. Ligthart, "Optimization of Metal Case of a Ground Penetrating Radar Antenna", *34th European Microwave Conference, Amsterdam*, Netherlands, p.p. 1257-1260, 2004.
[3] A. V. Vorobyov, A. G. Yarovoy, P. Aubry, and L. P. Ligthart, "Cavity-backed UWB Antenna for Impulse Radio Applications", *Proc. of 2nd EuCAP*, Edinburgh, U.K., 2007.

3.3 Radar processing

The processing chain of acquired radar data consists of pre-processing, focusing (imaging) and shape-based detection of targets in high-resolution 3-D radar images. One can find a detailed description of each stage in deliverables D14 and D18.

Pre-processing suppresses noise and removes non-informative components such as antenna coupling, unwanted reflections from background and radar impulse response out of the data. Band-pass finite impulse response filtering, subtraction of the stationary antenna coupling and time gating remove the parasitic components, while deconvolution compresses the target pulse and consequently it sharpens the radar image. As example, Figure 3-15 illustrates the pre-processing for a small metal sphere.

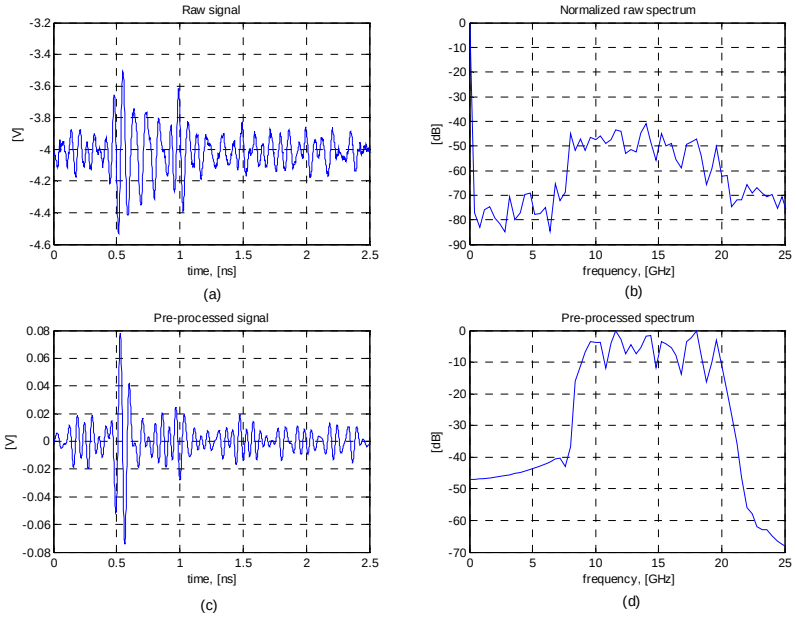

Figure 3-15: Pre-processing of reflection from a small metal sphere (4 cm diameter): (a)-(b) raw signal and spectrum, (c)-(d) pre-processed signal and spectrum

Focusing of data acquired by SAR, the MIMO array and combined MIMO-SAR systems is achieved by means of Kirchhoff migration which was extended to the specified systems. This imaging technique was selected on the basis of a comparative analysis carried out in D14. It provides the smallest level of artefacts in the imagery. Figure 3-16 illustrates a cross-range resolution capability of the MIMO array for two closely spaced metal spheres.

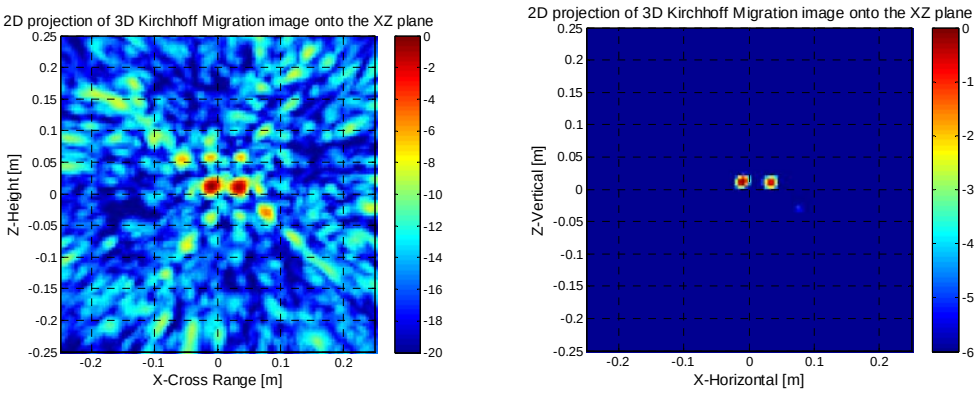

Figure 3-16: MIMO image of two metal spheres separated by 3 cm

(a) 20 dB dynamic range; (b) 6 dB dynamic range

Once the datasets have been focused they are further processed towards a shape-based classification algorithm. This is achieved using a GUI specially developed for RADIOTECT in four stages. The GUI was implemented to process the reconstructed data to a point where we can match the object's shape contours in order to digitally classify the measured object. The GUI exists out of four subGUIs that have been implemented to sequentially process different kinds of data:

- DataGUI: to read, select and transform the input data.
- LayerGUI: to scan through, divide and merge 3D data.
- FilterGUI: to filter and segment 2D data. Here a larger number of classic image processing and morphological filters are available.
- SnakeGUI: to build and analyze vectorial contour data, and perform the classification. The Snake algorithm delineates contours in the image and returns them in vectorial form. This form can then be used to make an object classification through comparing with a preset library of known object contours.

The GUI was developed to be used in a Matlab environment. The file GUISTART.m opens up the GUI from which the previously mentioned subGUIs can be properly accessed in an automatically Data-dependant appointed order. If desired, the separate subGUIs can also be called up individually, by running the corresponding filenames: GUI3DLayers.m, GUI2DFilter.m and GUI2DSnake.m in Matlab with an input dataset given as a function argument.
When proceeding from one subGUI to another, the newly accessed GUI will open up into a separate window. This helps research by creating the option for a tree-like traversing of processing possibilities. One can take two (or more) different processing paths from one previously acquired result, comparing these paths to find the more fitting. Figure 3-17 shows the 4 subGUI's in the processing chain of detecting a gun on a human chest.

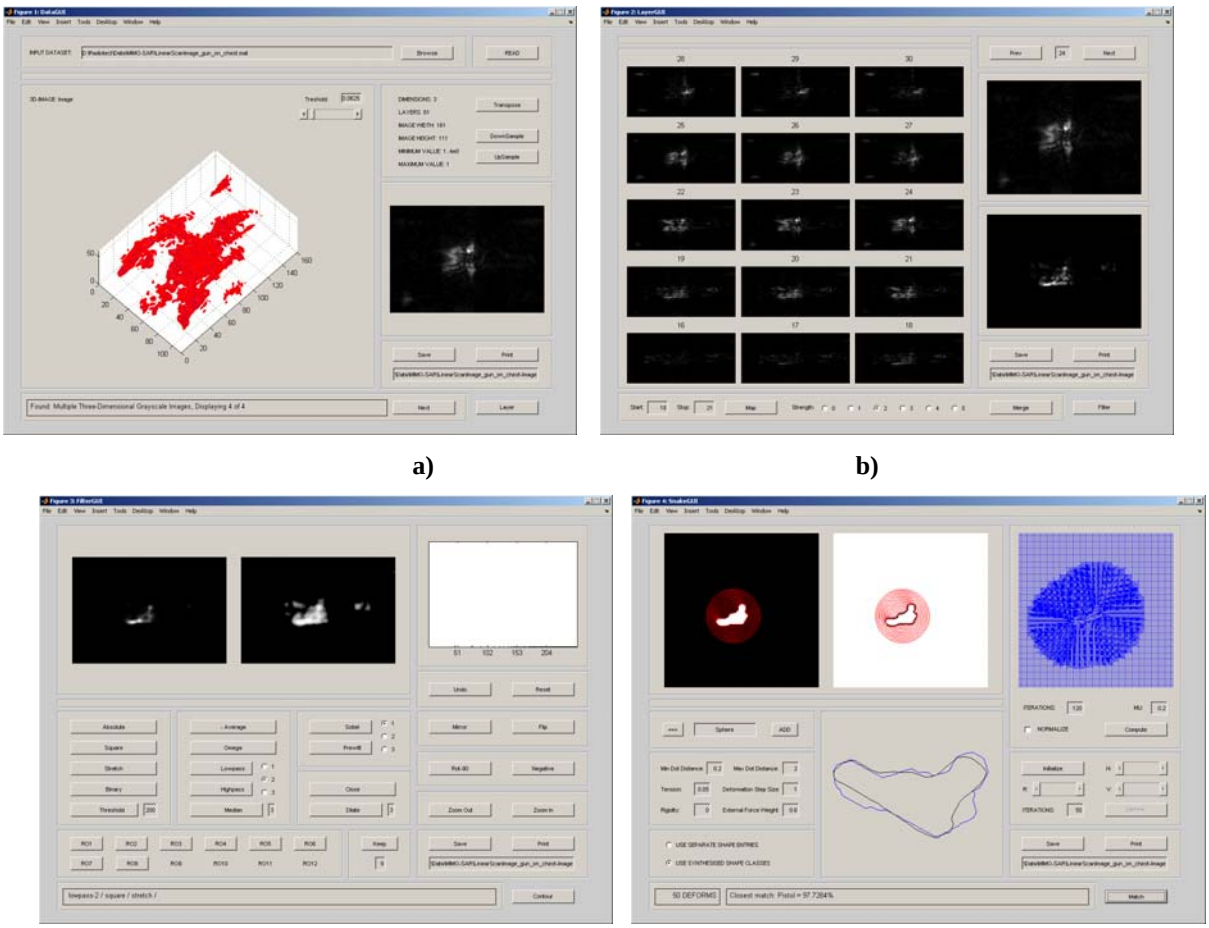

a) **b)**

c) **d)**

Figure 3-17: The final results for the 4 subGUI's for a dataset containing a gun on a human chest. (a) The data was read in and oriented correctly so as to find the best visualisation for the next step. (b) The layers with the highest energy are detected and combined to form one image containing the Gun information, rejecting the chest reflections. (c) A few simple filtering steps are applied on the image to enhance the gun form. (d) The Snake algorithm was successful in delineating the Gun's contours. The classification was performed and returned the class "pistol" with a certainty of 94%.

3.4 Examples

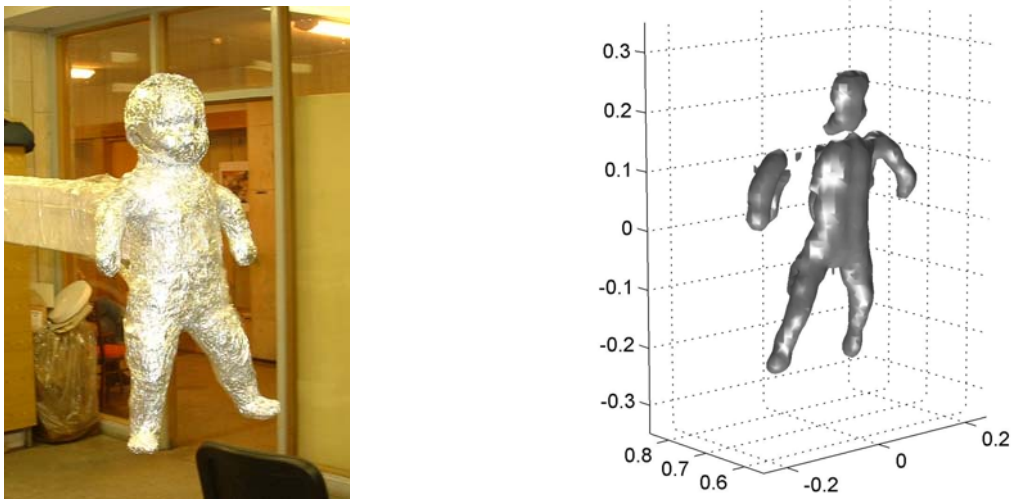

Figure 3-18: SAR imaging of a doll wrapped with metal foil in frequency band 3.1 – 10.6 GHz

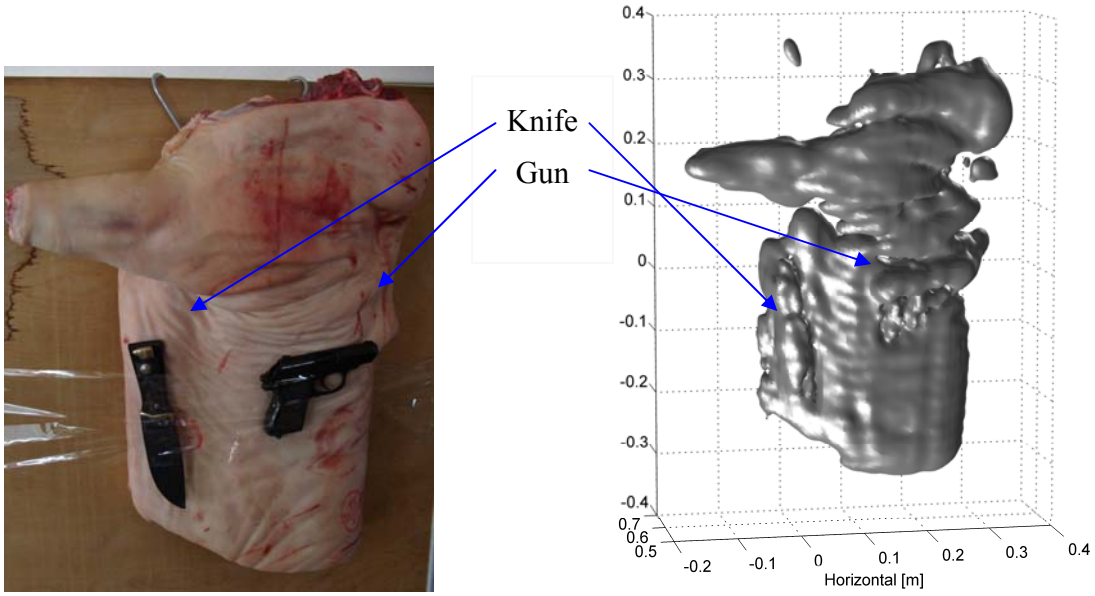

Figure 3-19: SAR imaging of an armed pig carcass n frequency band 3.1 – 10.6 GHz

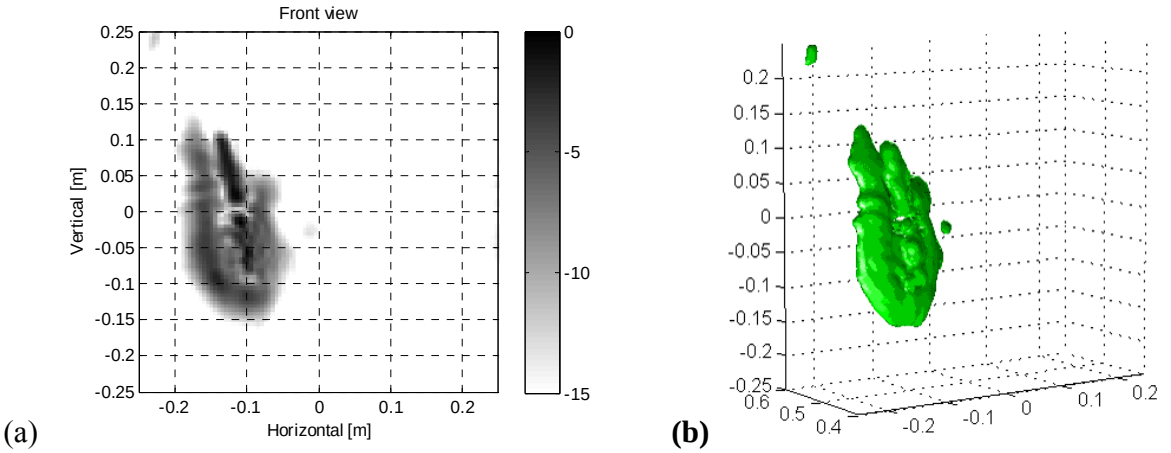

Figure 3-20: SAR imaging of a knife on pig leg in frequency band 10 -18 GHz

a) 2 D image; b) 3 D image

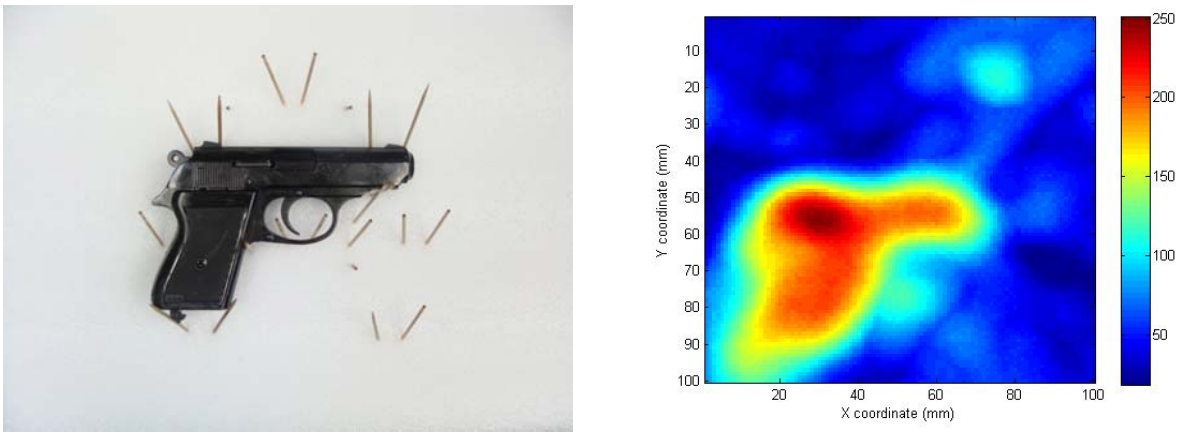

Figure 3-21: MIMO imaging of a gun in frequency band 3.1 -10.6 GHz.

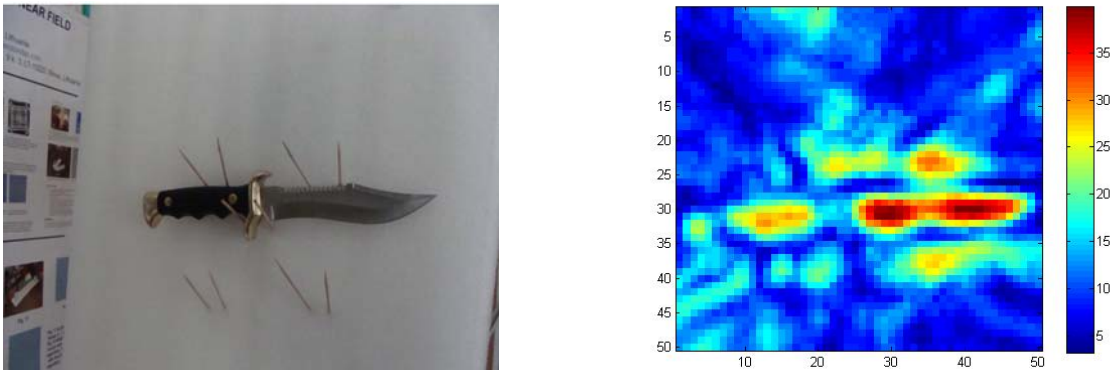

Figure 3-22: MIMO image of a knife in frequency band 3.1 -10.6 GHz.

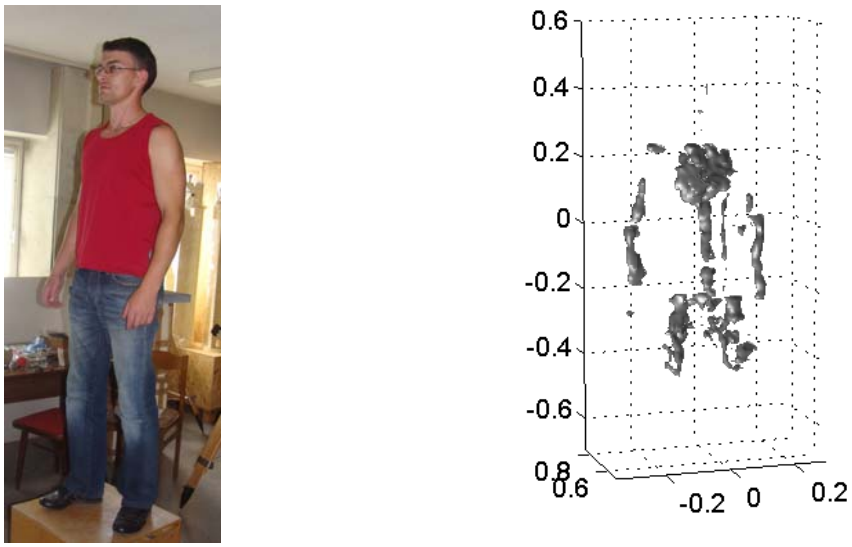

Figure 3-23: MIMO –SAR imaging of a standing man in frequency band 10 – 18 GHz

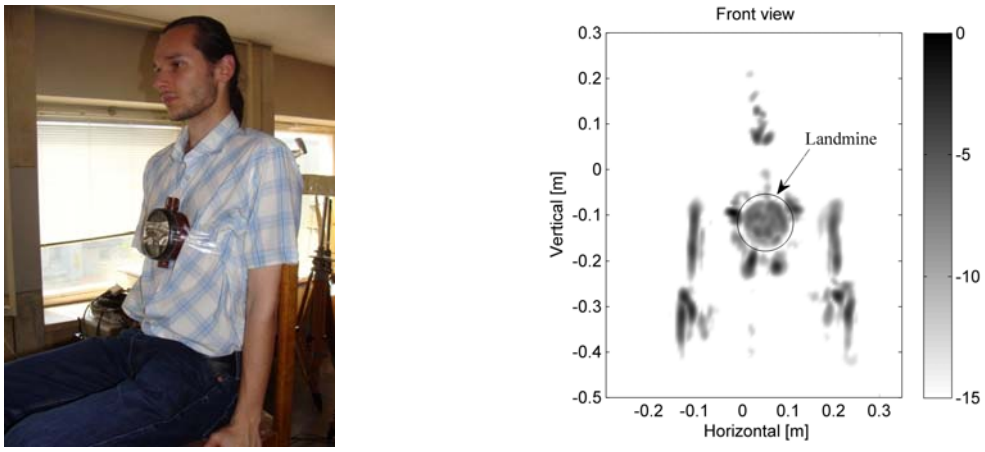

Figure 3-24: MIMO-SAR imaging of a man with plastic landmine in frequency band 10 – 18 GHz

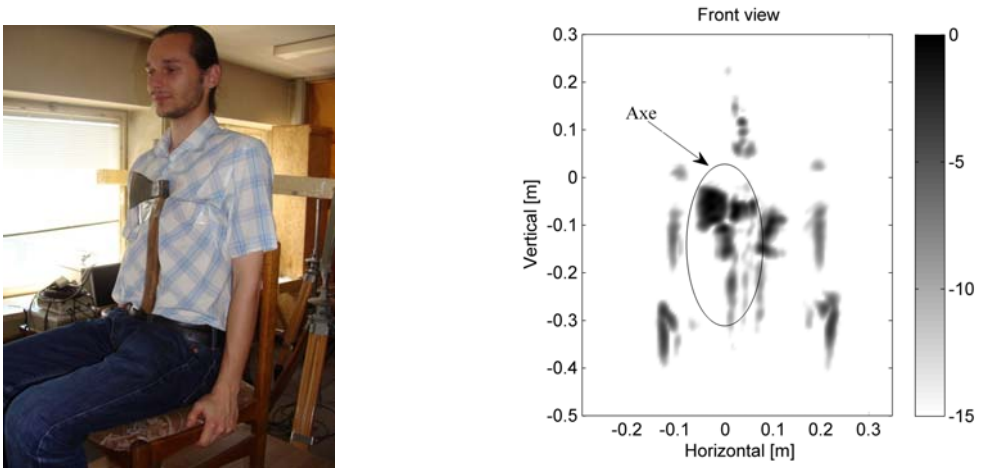

Figure 3-25: MIMO-SAR imaging of a man with axe with a wooden handle in frequency band 10 – 18 GHz

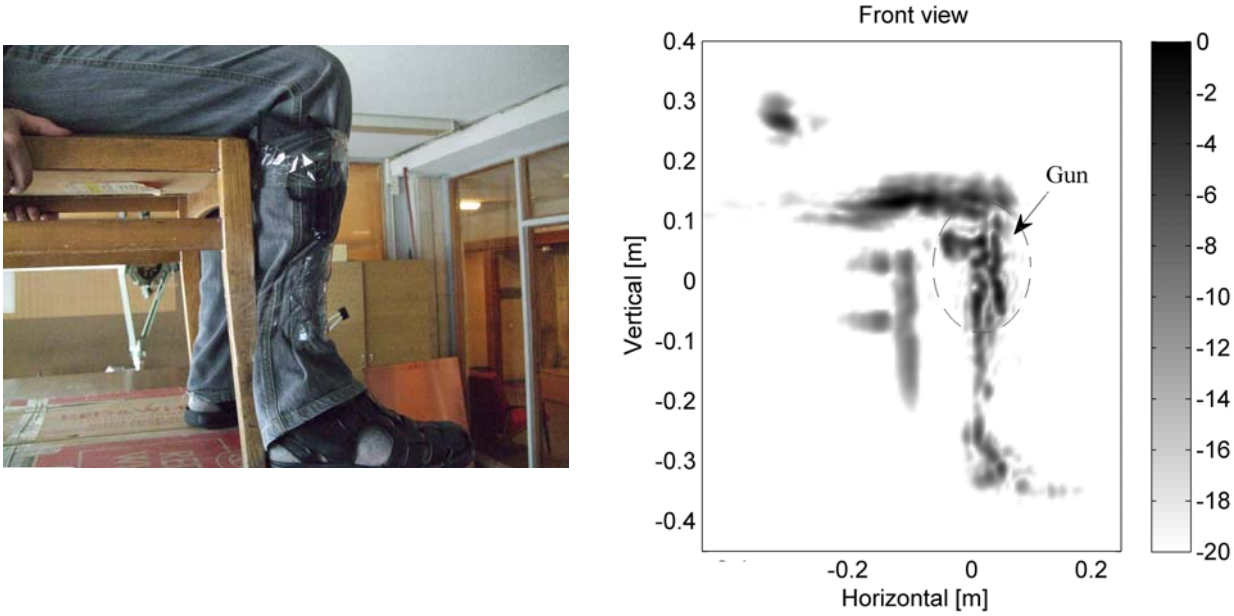

Figure 3-26: MIMO-SAR imaging of a man with gun on the knee in frequency band 10 – 18 GHz

4 Detection of buried people

4.1 How to detect buried people by radar?

The detection of buried people is based on two properties of radar sensors. First, the emitted radio waves are able to penetrate rubble even if it is riddled with metal parts (e.g. reinforced concrete) and second it is able to register very weak movements.

The penetration of rubble by radio waves depends upon their frequency. The lower it is, the better the wave can penetrate. On the other hand, the performance of localisation and movement detection improves with increasing bandwidth, respectively frequency. A reasonable compromise between penetration and localisation/detection is to operate in the frequency band of about 100 MHz to 2 GHz.

By propagating through the rubble, the sounding waves are scattered at any interface between two materials of different permittivity and conductivity. Hence, the human body will also cause such reflections which can be registered by the radar sensor. However, since in a collapsed building a great many of such interfaces exist and furthermore these interfaces are arbitrarily orientated in space, the back scattered signals are completely chaotic in structure so that one is possibly able to identify big objects with some chance but definitely not to detect a human being.

An exception is given for the case where the buried person is still alive. This point is of major interest for search and rescue operations, since an improved search strategy could save lives. From

the view point of a radar device there is however no difference between rubble and human beings with respect to the wave scattering except the human being is moving if alive and the rubble is not. If the person is not completely blocked, they can wave with the arms or legs, if blocked or unconscious at least the chest is moving due to breathing.

Figure 4-1 demonstrates the principle of how to detect a small movement by a radar sensor. If the target is shifted by a small distance, than the roundtrip time will change a little. This is translated into weak variations of voltage samples which are located at an edge of the backscattered signal. The smallest voltage variation verifiable by the radar sensor and the data processing will determine the sensitivity to detect buried people. Only the data point located at the signal edges are of interest here, hence the signal perturbations due to random noise and jitter should be as low as possible.

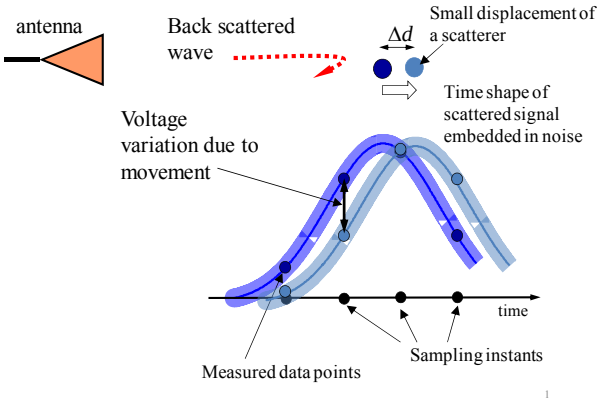

Figure 4-1: Principle of movement detection by a radar device

Under real conditions, the backscattered signal is not only composed of a single edge as demonstrated in Figure 4-1. Rather it is constituted from several oscillations as illustrated in Figure 4-2. Unfortunately, it is not possible to predict the shape of that signal because the transmitted waveform will be largely disrupted on its way through the rubble.

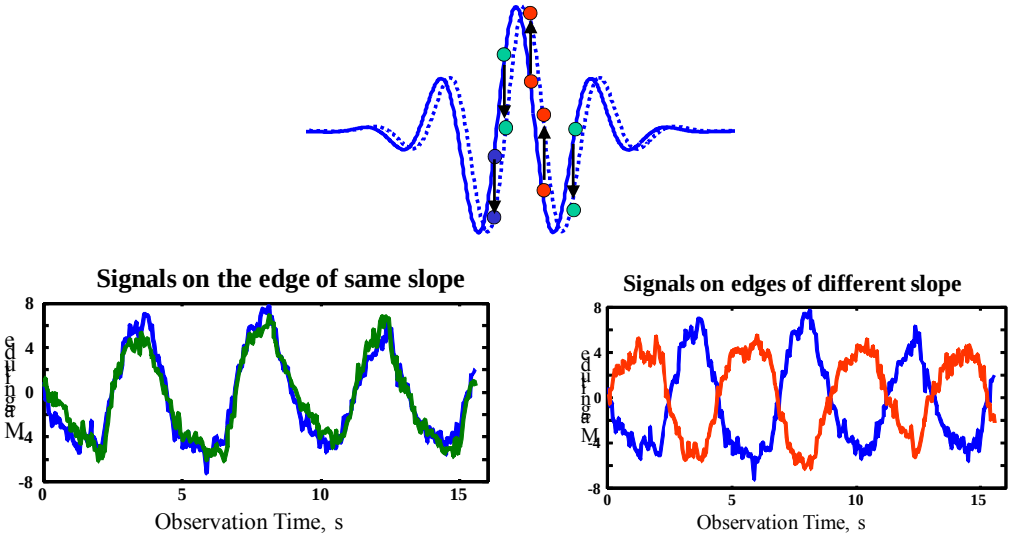

Figure 4-2: Simplified shape of a backscattered signal and the voltage variation of different samples due to a small shift of the target (above). Measured voltage variation of some samples due to breathing of a person (below).

Radar devices using narrow band signals (in the extreme case this can be a Doppler radar) are also able to detect very small movements of a target. Their signal will not be disrupted by the rubble due to its large spatial extension. This simplifies the data processing. However, due to their lower spatial resolution, these radar devices are less able to exactly localise a victim and more importantly they are sensitive to foreign targets which move as well.

4.2 The radar device

The radar electronics is based on the digital ultra wideband M-Sequence approach. The block schematic of the radar device is depicted in Figure 4-3. The operational frequency band of the radar system extends from about 60 MHz to 2.5 GHz. The M-sequence approach is a very time stable radar principle which promotes the detection of weak movements due to its excellent jitter performance.

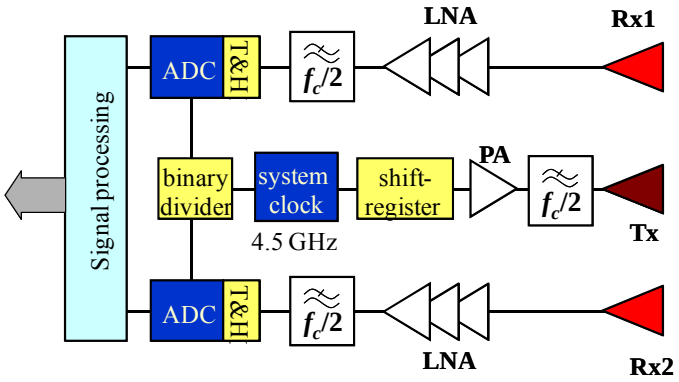

Figure 4-3: Block schematics of the radar device

The antennas are comparatively large spiral antennas. Their size is determined by the required low cut-off frequency. Figure 4-4 shows a photograph.

Figure 4-4: Photographs of the antennas

The radar device consists of one transmit and two receive channels. For the basic operation, one receive channel would be sufficient. However, the more channels the radar has the larger the coverage of the search area and the simpler the victim localisation.

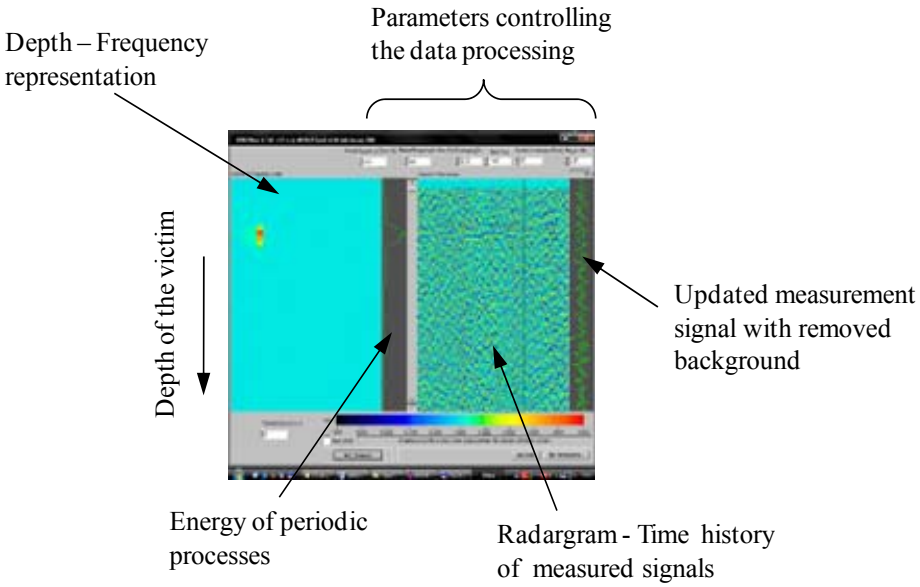

Figure 4-5: Screen shot of the GUI applied for search and rescue of trapped people.

The operation of the radar device is managed remotely in order to avoid perturbations by the proper motion of the operator. By a GUI, some parameters to control the data processing can be adjusted. Four screens represent the data. From right to left, we have:

- Measurement update: It updates permanently the current measurements. The indicated trace is removed from stationary background caused from the scattering of rubble.
- Radargram: It represents the time history of measured data from which the background was removed. This screen can be used to identify arbitrary motions (as e.g. waving with hands). In such a case a horizontal trace is visible at a certain distance respectively depth.
- Energy of periodic processes: It represents the horizontal integral of the time-frequency representation and serves to detect periodic events.
- Depth-frequency representation: Weak target movements are covered by noise in the radargram. If these movements are periodic as e.g. breathing, they can be enhanced from noise by their frequency respectively by their repetition rate. Thus, an object which is located at a certain depth and periodically changes its body shape will give a blob on the screen.

4.2.1 GEOZONDAS system for vital data capturing and monitoring through wall and through rubbles

GEOZONDAS concentrated mainly on the TDI investigations in the project, but it was also able to adapt its technology to provide vital data and to compare the results with the M-Sequence device. The system (Figure 4-6) was designed by GEOZONDAS. Live being detection is based on

detecting change in the reflected signals. If the man is moving, the difference is represented with a strong spike. The breathing spectrum is measured, when the man is immovable.

The system includes:

- 2-channel Sampling Converter
- Pulse Generator mainframe and generator heads with FWHM 30 ps or 100 ps
- 2 UWB Antennas with frequency band 1-30 GHz, 3.1 – 10.6 GHz or 0.5 – 2.5 GHz.
- Software developed in Geozondas , MARCHA 2008.

(a)  (b) 

Figure 4-6: Geozondas radar system

a) Indoor breathing and hearth beating monitoring ; b) Outdoor live being detection through rubbles

4.3 Examples

In what follows, the detection performance and procedure is demonstrated by two examples. The first one is shown in Figure 4-7. It refers to the detection of a trapped person located on the floor of the basement in a building. During the measurement, no other person was inside the building. The Radar device was located on the 3rd floor (about 13 m above the victim). The person could not be detected in the radargram but in the depth-frequency representation he was clearly visible.

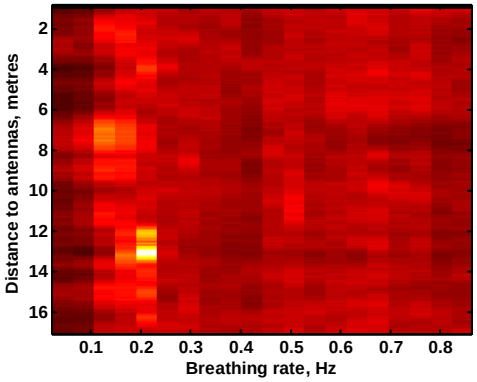

Depth-frequency representation

Figure 4-7: Detection of a trapped person in a building

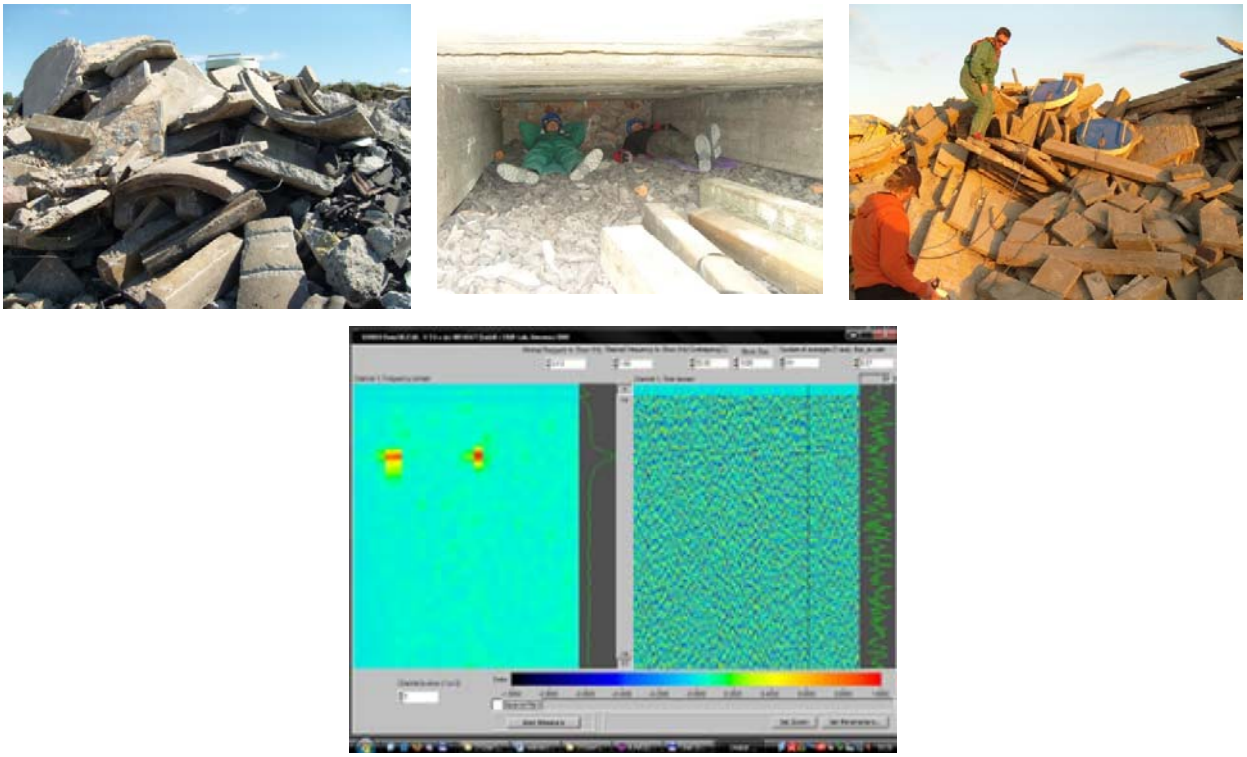

Figure 4-8: Detection of people beneath rubble.

The second case deals with the detection of people beneath rubble. The example shown in Figure 4-8 relates to heavy rubble consisting of reinforced concrete which complicates the penetration of

electromagnetic waves due to their metal content. Nevertheless, the victims could be detected down to 1.7 m of compact rubble.

For test purposes, the victims were hidden in a cave beneath the rubble and the antennas were placed on top. The victims were asked to breath with different rates. This could be observed in the depth-frequency representation of the radar device (see Figure 4-8). As visible in that figure, the simple radargram representation was meaningless in that example because all signal components caused by the breathing motion are covered by noise.

In all cases, (as also depicted here) the actually captured data does not show the presence of hidden persons since the strong reflection from the rubble covers the reflection from the human body. Figure 4-9 gives an example.

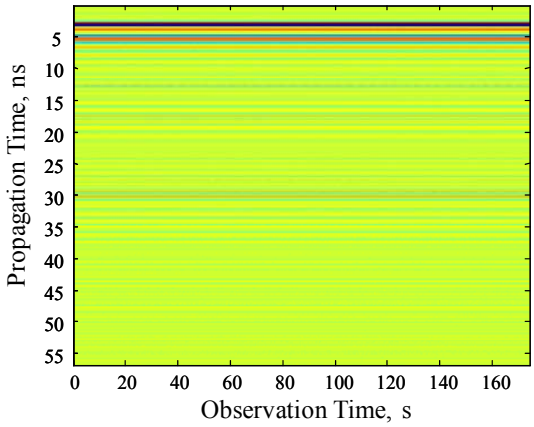

Figure 4-9: Actually captured data represented by a radargram.

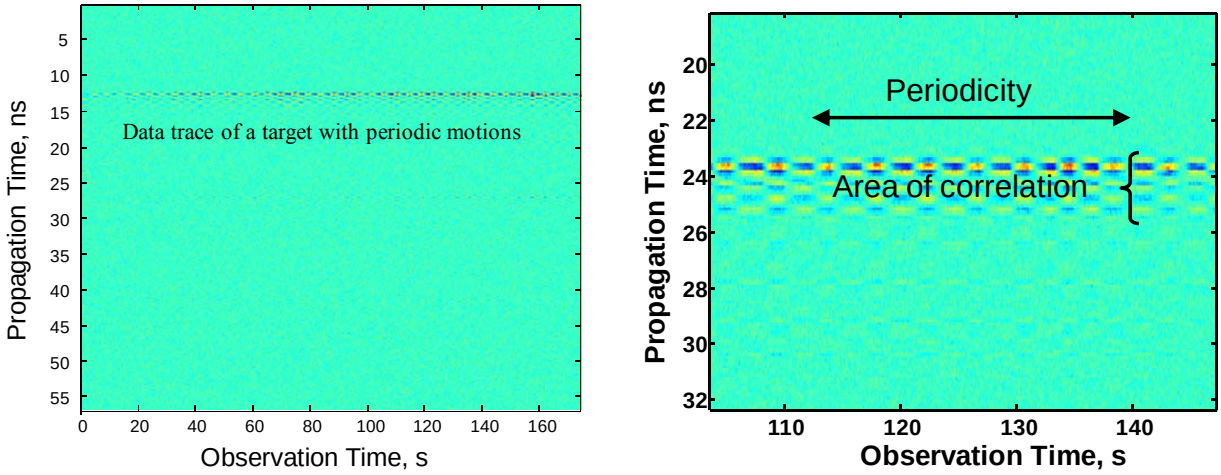

Figure 4-10: Enhancement of backscatter components from a target in periodic motion. The graph on the right is a zoomed version of the original data on the left.

By removing the stationary reflections from the measured signal, the movements of a target become visible as depicted in Figure 4-10. If the scattering object executes a periodic motion, this will be reflected by the signal structure in the observation time direction. We can even identify a whole "breathing band" in the radargram over which this periodicity can be observed. Unfortunately, the signal structure in the propagation time direction of that "breathing band" is less obvious. It is largely influenced by the structure of the rubble and it cannot be predicted beforehand.

The measurement conditions leading to the radargram in Figure 4-10 were far from the complicated conditions as demonstrated in Figure 4-7 or Figure 4-8. Under these constraints, the resulting radargram looks like that from Figure 4-11. Obviously, noise and perturbations by radio stations will also cover the target of interest.

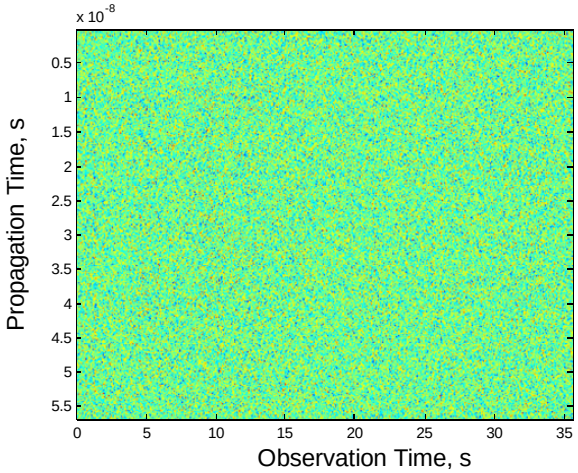

Figure 4-11: Radargram of a moving scatterer at a large depth after removing stationary backscattering

Hence, further strategies to enhance the target motion must be applied. In the case of breathing detection, its periodicity in time can be used to suppress noise and furthermore, one can run a search procedure which locks on the unknown signal structure in the propagation time direction. Figure 4-12 illustrates the result of such a procedure. Now, the victim is visible. The noise suppression by that approach is increased by extending the observation time. A reasonable duration for an observation covers a couple of minutes.

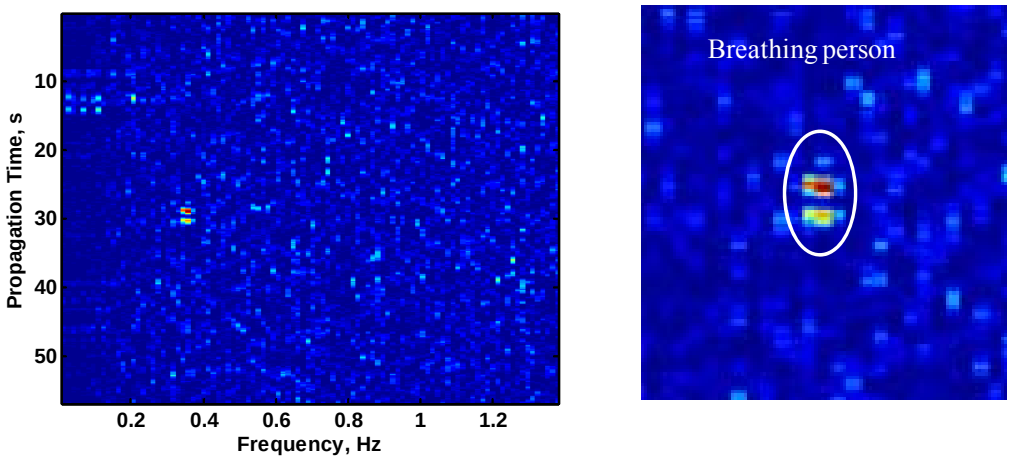

Figure 4-12: Enhancement of periodic motions in the depth-frequency domain. The picture on the right is a zoomed version of the complete data set.

Figure 4-13 and Figure 4-14 present examples of results achieved with the GEOZONDAS system in the project described under 4.2.1.

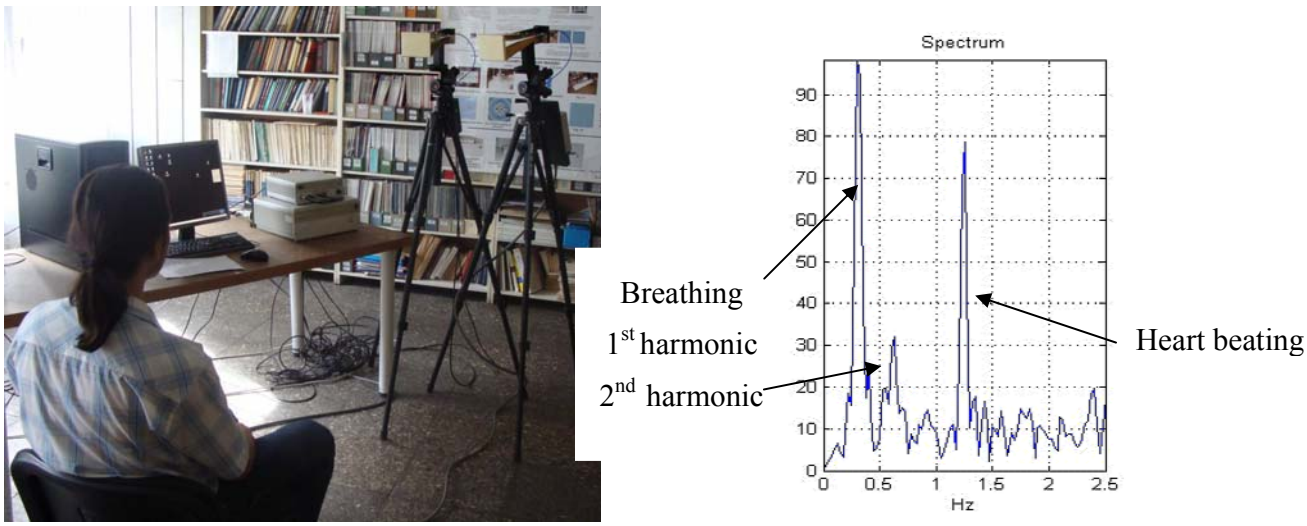

Figure 4-13: Breathing and heart beating spectrum measurement in frequency band 1 -30 GHz

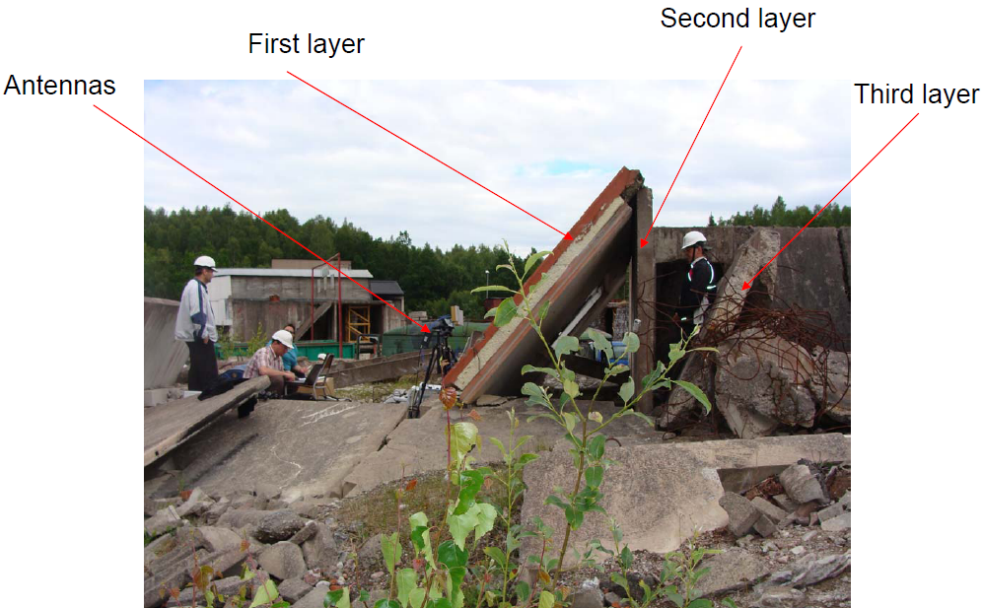

(a)

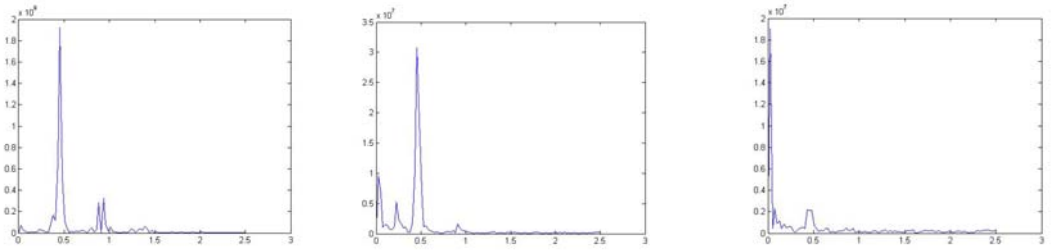

(b) (c) (d)

Figure 4-14: Human breathing detection through rubbles in frequency band 0,5 – 2.5 GHz

Breathing frequency 0.4 Hz. (a) Scenario; (b) Spectrum measured through 1st layer; (c) Spectrum measured through 2 layers; (d) Spectrum measured through 3 layers.

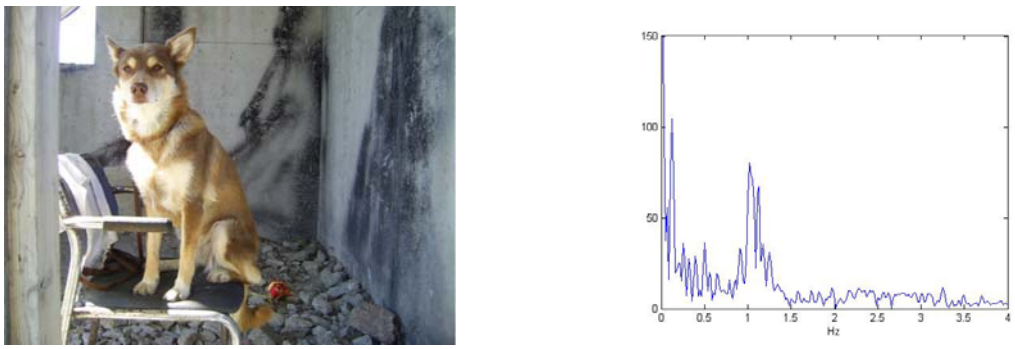

Figure 4-15: Dog breathing detection through wall in frequency band 0,5 – 2.5 GHz

a) Breathing frequency 1.1 Hz

5 Conclusions

The project has been successful in meeting its overall objectives of:

- Developing high and ultra high resolution radar hardware for the detection of hidden persons / objects for use in rescue and security applications
- Developing imaging techniques and algorithms for use with high and ultra high resolution radar for the detection and localisation of persons / objects for rescue and security applications
- Testing the above technologies to help determine methodologies of use and room for further improvements.
- Improve the competitiveness of the SMEs in the project and the establishment of transnational cooperation
- Promote the technology to strengthen its commercial success.

Specifically:

- A high resolution radar working with the M-Sequence technique has been developed to enable security forces to detect persons hidden behind walls. This was achieved through advances in the state of the art for radar electronics and algorithms for person detection and tracking.
- A high resolution radar also working with the M-Sequence technique has been developed for to enable rescue forces to detect persons trapped under rubble. This was also achieved through advances in the state of the art for radar electronics and algorithms for person detection and localisation.
- A further high resolution radar working with the sub-nano second impulse technique has been developed which demonstrates the ability to detect movement including heart beat and breathing also for security or rescue applications. This was also achieved through advances in the state of the art for radar electronics and algorithms for person detection and localisation.
- 3 systems working with the sub-nano second impulse radar technique up to 18 GHz were developed to investigate the challenge of imaging objects hidden behind clothes. This was also achieved through advances in the state of the art for radar electronics and algorithms for person detection and localisation.
- Components were developed utilising SiGe semiconductor chip and LTCC technology for a mm-wave radar to work in the frequency range 60-70 GHz. This was also achieved through advances in the state of the art for radar electronics.
- All systems have been tested in the laboratory and those closest to the market evaluated in tests with end users.
- The SMEs have results from the project which they assess as increasing their competitiveness. The SMEs estimate their economic benefit from the project will be as high if not higher than planned in preparing the project.

- Products for rescue and security application are foreseen and project results may be used in other application areas.
- The partners have developed strong and trusting working relationships with each other.
- There have been 41 scientific papers published (or will be published) at the time of writing on results from the project.